Real-Time Risk Assessment and Management of Pipelines

Spring 2002 Report

To

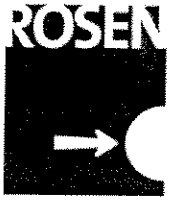

H. Rosen
Engineering

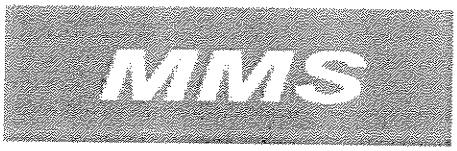

Minerals Management Service

By

Professor Robert Bea
&
Graduate student researcher Ziad Nakat

Marine Technology & Management Group
Department of Civil & Environmental Engineering
University of California at Berkeley

Table of Content

I) Introduction

1. Objective

The objective of this project is to develop, verify, and test procedures that can be used during the in-line instrumentation of pipelines to characterize their reliability (probability of not loosing containment). This project is sponsored by the U.S. Minerals Management Service (MMS) and ROSEN Engineering.

2. Scope

The Real-Time RAM (Risk Assessment & Management) of Pipelines project is addressing the following key aspects of criteria for in-line instrumentation of the characteristics of defects and damage in a pipeline.

1) Development of assessment methods to help manage pipeline integrity to provide acceptable serviceability and safety,

2) Definition of reliabilities based on data from in-line instrumentation of pipelines to provide acceptable safety and serviceability,

3) Development of assessment processes to evaluate characteristics of in-line instrumented pipelines,

4) Evaluation of the effects of uncertainties associated with in-line instrumentation data, pipeline capacity, and operating conditions,

5) Formulation of analysis of pipeline reliability characteristics in current and future conditions,

6) Validation of the formulations with data from hydrotesting of pipelines and risers provided by the POP (Performance of Offshore Pipelines) project.

7) Definition of database software to collect in-line inspection data and evaluate the reliability of the pipeline.

Important additional parts of this project provided by ROSEN engineering and MMS will be:

1) Provision of in-line instrumentation data and field operations data to test the real-time RAM formulations,

2) Conduct of workshops and meetings in Lingen, Germany and UCB to review progress and developments from this project and to share technologies,

3) Provision of a scholarships to fund the work of graduate student researchers that assist in performing this project, and

4) Provision of technical support and background to advance the objectives of the project.

3. Approaches

The fundamental approach used in this project is a Risk Assessment and Management (RAM) approach. This approach is founded on two fundamental strategies:

- Assess the risks (likelihood and consequence) associated with existing pipelines, and

- Management the risks so as to produce acceptable and desirable quality in the pipeline operations.

It is recognized that some risks are knowable (can be foreseen) and can be managed to produce acceptable performance. Also, it is recognized that some risks are not knowable (cannot be foreseen), and that management processes must be put in place to help manage such risks.

Applied to development of criteria for the requalification of pipelines, a RAM approach proceeds through the following steps (Bea, 1998):

1) Based on an assessment of costs and benefits associated with a particular development and generic type of system, and regulatory – legal requirements, national requirements, define the target reliabilities for the system. These target reliabilities should address the four quality attributes of the system including serviceability, safety, durability, and compatibility,

2) Characterize the physical conditions (e.g. corrosion, dents, gouges, and cracks), the internal conditions (e.g. pressures, temperatures), and the operational conditions (e.g. installation, production, and compatibility) that can affect the pipeline during its life,

3) Based on the unique characteristics of the pipeline system characterize the 'demands' (imposed loads, induced forces, displacements) associated with the environmental and operating conditions. These demands and the associated conditions should address each of the four quality attributes of interest (serviceability, safety, durability, and compatibility),

4) Evaluate the variability's, uncertainties, and Biases (different between nominal and true value) associated with the demands. This evaluation must be consistent with the variability's and uncertainties that were included in the decision process that determined the desirable and acceptable target reliabilities for the system,

5) For the pipeline system define how the elements will be designed according to a proposed engineering process (procedures, analyses, strategies used to determine the structure element sizes), how these elements will be configured into a system, how the system will be constructed, operated, maintained, and decommissioned (including Quality Assurance – QA, and Quality Control – QC process),

6) Evaluate the variability's, uncertainties, and Biases (ratio of true or actual values to the predicted or nominal values) associated with the capacities of the pipeline elements and the pipeline system for the anticipated environmental and operating conditions, construction, operations, and maintenance activities, and specified QA – QC programs. This evaluation must be consistent with the variability's and uncertainties that were included in the decision process that determined the desirable and acceptable target reliabilities for the system.

It is important to note that several of these steps are highly interactive. For some systems, the loadings induced in the system are strongly dependent on the details of the design of the system. Thus, there is a potential coupling or interaction between Steps 3, 4, and 5. The assessment of variability's and uncertainties in Step 3 and 5 must be closely coordinated with the variability's and uncertainties that are included in Step 1. The QA – QC processes that are to be used throughout the life-cycle of the system influence the characterizations of variability's, uncertainties, and Biases in the capacities of the system elements and the system itself.

4. The Project Premises

The design criteria and formulation developed during this project are conditional on the following key premises:

1) The design and analytical models used in this project will be based on analytical procedures that are derived from fundamental physics, mathematics, materials, and mechanics theories.

2) The design and analytical models used in this project will be found on analytical procedures that result in un-biased assessment of the pipeline demands and capacities.

3) Physical test data and verified and calibrated analytical model data will be used to characterize the uncertainties and variability's associated with the pipeline demands and capacities.

4) The uncertainties and variability's associated with the pipelines demands and capacities will be concordant with the uncertainties and variability's associated with the background used to define the pipeline reliability goals.

5. Project Tasks

The principal tasks defined for the conduct of this project are:

1) Develop, verify, and test procedures that can characterize the reliability upon the results from in-line instrumentation with various features including corrosion, cracks, gouges, dents, etc.

2) Evaluate available data from in-line instrumentation including the uncertainties associated with pigging tool itself and its specification.

3) Evaluate the uncertainties associated with in-line inspection data, pipeline demands (operating conditions), and capacities using simplified reliability based method.

4) Develop formulations to analyze reliability of pipeline in current condition. The consequence of pipeline failure will be included.

5) A parallel project will be utilized to verify the analytical procedures developed during this project.

6) Summarize comprehensively how to utilize this project into practical operations and service in the industry.

7) Document the forgoing results in four project phase reports

8) Transfer the forgoing results to project sponsors in five project meetings

6. Current research phase tasks.

1) Literature review on inspection techniques, associated uncertainties of detection/non detection, reliability methods, and prediction models for evaluation of burst pressures.

2) Evaluate in line inspection uncertainties and develop required calculations and Excel spreadsheets for this evaluation.

3) Develop Excel spreadsheets to integrate these uncertainties for the calculation of the probability of failure.

4) Modify predictive models to account for inspection uncertainties.

5) Develop guidelines for the use of all developed spreadsheet during this project.

6) Test the developed models with the use of a numerical example.

7) Analyze results.

8) Recommendation for proper understanding of inspection uncertainties for engineers.

9) Appendixes including spreadsheets calculations.

II) Literature review

A) Previous reports

1.1 Introduction

As the pipeline infrastructure system ages, it is important that pipeline operators have the technology to inspect and assess the state of their pipelines. Information on inspection techniques can be found in literature.

1.2 Fundamentals of In-Line Instrumentation

An intelligent pig, or a 'smart pig,' or in-line inspection tool, is a self-contained inspection tool that flows through a pipeline with the product. Pipeline operators use smart pigs to evaluate the integrity of transmission pipelines. Smart pigs, or in-line inspection tools, inspect the full thickness of the pipe wall. These tools are designed to look for conditions such as metal-loss corrosion, cracks, gouges, and other anomalies. The two main objectives of smart pigs are to detect potential defects, and then determine the size of the detected defect.

It should be noted that detection requirements depend upon the overall goal of the pipeline inspection. One operator may be interested in using inspections to uncover problem areas in a pipeline; hence the objective of the inspection is to locate defects in the initial stages of their growth life. Another operator may want to ensure that their lines have no defects, which threaten pipeline integrity; therefore, they are interested in larger (d/t>50%) defects only (Bubenik, 2001).

According to Batelle, magnetic flux leakage (MFL) is the oldest and most commonly used in-line inspection method for pipelines. The magnetic flux leakage technique provides an indication of the general condition of a pipeline section. MFL is a mature technique, extensively used in self-contained smart pigs. A permanent magnet generates a magnetic field in the pipe wall, so that a reduction in material will cause flux to leak. Most of the magnetic flux field lines pass through the pipe wall. The pipe wall is the preferred path for the flux. In the region of metal-loss region, the sensor records a higher flux density or magnetic field, thus indicating the presence of an anomaly. Furthermore, defects distort the applied magnetic field, producing flux leakage. The amount of flux leakage depends on the size and shape of the defect, as well as the magnetic properties of the pipeline steel. Sensors measure flux leakage, and record the measurements inside the pig. The measurements taken by the pig are analyzed after the inspection is completed to estimate the defect geometry depth.
An MFL pipeline inspection tool is a self-contained unit, containing magnets, sensors, data recording systems, and a power system. The systems used in most MFL tools include:

- A drive system, which uses the pressure differential in the pipeline to propel the tool.

- A power system, which provides battery power for the sensors, and data recording system.
- A magnetization system for magnetizing the pipe.
- A sensor system to measure the flux-leakage signal.
- A data recording system, which amplifies, filters, and stores the measured signals (Bubenik, 2001).

Figure 1.2.1: Layout of Components of MFL Pipeline Pig (www.phy.queensu.ca)

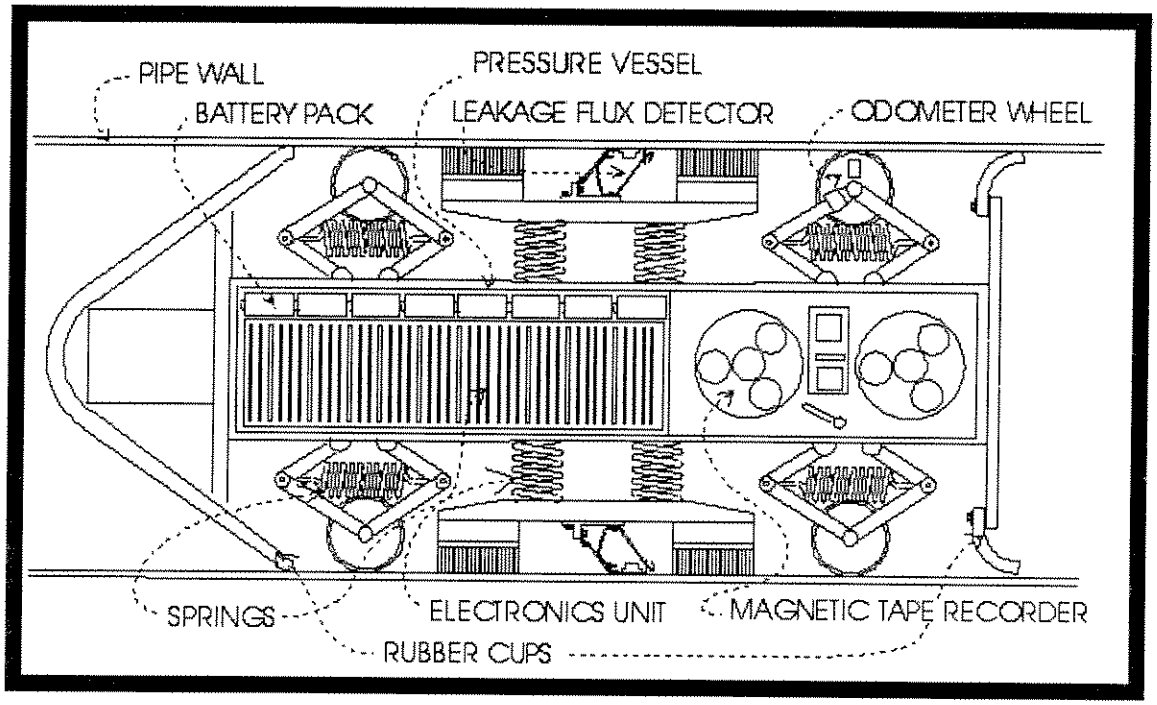

1.3 Performance Specifications for In-Line Instrumentation

1.3.1

Manual Analysis:
(Applicable for detailed analyzed features)

POD = Probability of Detection

	General Defect	Pitting Detect	Axial Grooving	Circumferential Grooving
Depth at POD = 90% (in fraction of t)	0.1	0.2	0.15	0.15
Depth sizing accuracy at 80% Confidence in -/+ fractions of t	±0.1	±0.15	±0.13	±0.11
Width sizing accuracy at 80% confidence in -/+ X mm	±15	±15	±10	±10
Length sizing accuracy at 80% confidence in -/+ X mm	±15	±15	±10	±10

Automatic Analysis:

	General Defect	Pitting Detect	Axial Grooving	Circumferential Grooving
Depth at POD = 90% (in fraction of t)	0.2	0.2	0.3	0.2
Depth sizing accuracy at 80% Confidence in -/+ fractions of t	±0.15	±0.15	±0.25	±0.15
Width sizing accuracy at 80% confidence in -/+ X mm	±25	±25	±15	±15
Length sizing accuracy at 80% confidence in -/+ X mm	±25	±25	±15	±15

Wall Thickness Detection:

± 1mm or ± 0.1t, whichever value is greater at 80% confidence.

1.3.2 Location and Orientation Capabilities

a. Axial position accuracy from reference marker: ± 1m
b. Axial position from closest weld: ± 0.1m
c. Circumferential position accuracy: ± 10°

1.3.3 Defect Dimension Definition

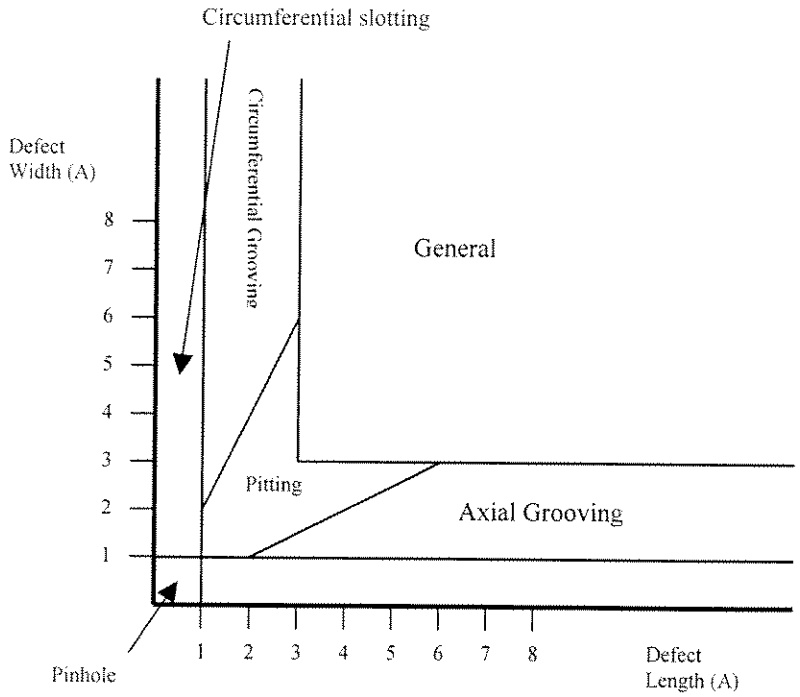

Note: t = wall thickness or 10mm, whichever value is greate

1.3.4 Identification of Features

POI: Probability of Identification

Feature	Yes POI > 90%	No POI < 50%	May be 50%<POI<90%
Internal/External discrimination	X		
Metal loss corrosion defect	X		
Metal loss pipe mill defect	X		
Midwall defect			X
Grinding			X
Gouge			X
Dent	X		
Spalling	X		
Axial crack		X	
Circumferential crack	X		
Eccentric pipeline casing			X
Sleeve repair	X		
Fitting	X		
Valve	X		
Tee	X		

From above table, it can be that the probability of longitudinal cracks is less than 50%.

2. Probability of Detection

2.1 Factors

There are four contributing factors, which directly influence the probability of detection of an MFL inspection tool (Beuker, 2001):

1. Inspection Tool Capability: mechanical parameters, such as magnetization level and configuration.

2. Calibration of Inspection Tool: defect population should be taken into account in calibration.
3. Interpretation of Results: interpreting the data printouts provided by the intelligent pig.

4. Defect Population: Adjacent defects make signal analysis difficult because the leakage fields overlap and affect each other.
    a. Distribution of depth.
    b. Noise Level
    c. Noise Parameter

2.2 Inspection Tool Capability: Mechanical Limitations

The characterization accuracy, including the probability that the pig will simply detect a metal-loss defect (POD), is related to the mechanical properties of the pig. For example, applied magnetic field strength produce stronger leakage fields, which improve the performance of the pig's detection and characterization abilities. The applied flux density in a pipe also depends upon the coupling efficiency between the magnet, the pipe, and on the local wall thickness. For the same applied magnetic field, an increase in wall thickness decreases the flux density in the pipe. Therefore, the strength of the magnetization system must be tailored to the wall thickness of the pipe to be inspected. Thick-walled pipe requires a larger magnetization (magnet) level in order to achieve saturation. Furthermore, variations in the wall thickness will change the applied field strength. Flux density is also a function of the local permeability of the pipe. Small changes in carbon content, alloying elements, and impurities create variations in permeability. The magnetization level strongly affects both detection and characterization accuracy. Magnet strength and magnetic coupling have the strongest affect on the applied field. Velocity, stress, repeated magnetizations of the line-pipe, and changes in the material properties of the pipe along the length of the pig run also affect the applied magnetic field. Ideally, the magnetization system in an MFL tool should produce a magnetic field that is strong enough to cause a measurable amount of flux leakage at defects; uniform from the inside surface to the outside surface of the pipeline wall thickness, and consistent in magnitude along the length of a pipe, so that measurements can be compared at different locations during an inspection run.

Sensors located on-board the pig convert the magnetic flux leakage field measurements into electrical signals that can be stored, analyzed, and reviewed. The sensor must optimize the information that it collects, as it balances the quantity and quality of the data that it collects. Sensors are spring-loaded against the pipe surface, allowing the sensors to ride over weld beads, dents, and debris. The stiffness of the mounting system and the mass of the sensors affect how closely the sensors ride the internal pipeline wall. A sensor wear plate protects the sensor from damage but provide a built-in stand-off between the sensor and the pipe wall, which affects POD. Furthermore, sensors filter the incoming data, and the size of the sensor affects the resolution of the system. Important sensor parameters include circumferential width of the sensor, sensor type, its axial position between magnet poles, and the ability of the sensor to reduce background noise levels (Bubenik, 2001).

Data storage devices located on–board the pig require battery power to operate. Therefore, the available battery power limits the mileage that can be inspected at any time. The power system is constrained by the size and shape of the interior of the inspection tool.

2.3 False Pig Calls

False pig calls are indications of defects in the collected data, where no defect actually exists. Two common causes of false calls are metal objects near the pipeline, and pipeline repair sleeves (Bubenik, 2001). False pig calls can lead to costly excavations,

and repair work being performed, without it being needed. The rate of false calls is related to the interpretation and use of the inspection results. If all indications of defects are to be excavated, the number of false calls should be minimized.

2.4 Definitions:

***Actual Decision Tree*:**

1. Pig call: a pipeline anomaly detected and recorded in the data of the instrumented pipeline, which may or may not actually exist.
2. Defect: an undesirable property of a pipeline, capable of being identified and measured by an intelligent pig.
3. Defect Classes*:
    a. Class I: corrosion pit
    b. Class II: pipeline dent
    c. Class III: pipeline gouge
    d. Class IV: combination of any of the above classes of defects
4. POD: Probability of detection
5. POI.X: Probability of identification of a given class of defect.

* Class I defects (corrosion) are the only defect types capable of being predicted, given that the defect is not detected by the pig.

Ideal Decision Tree:**

1. POF: Probability that the detected defect actually exists.
2. POM: Probability of missing an existing defect

** The ideal decision tree will not be used at this time for the real-time probability of failure calculation. The ideal decision tree requires data that does not yet exist.

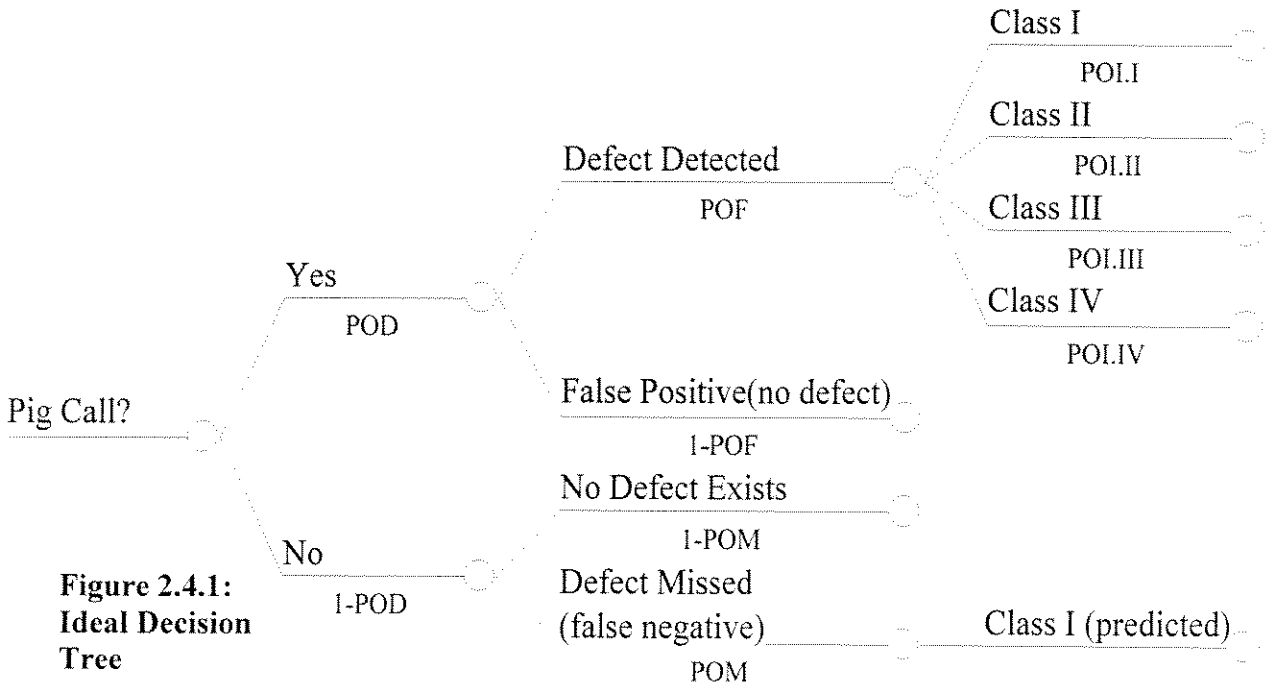

Figure 2.4.1: Ideal Decision Tree

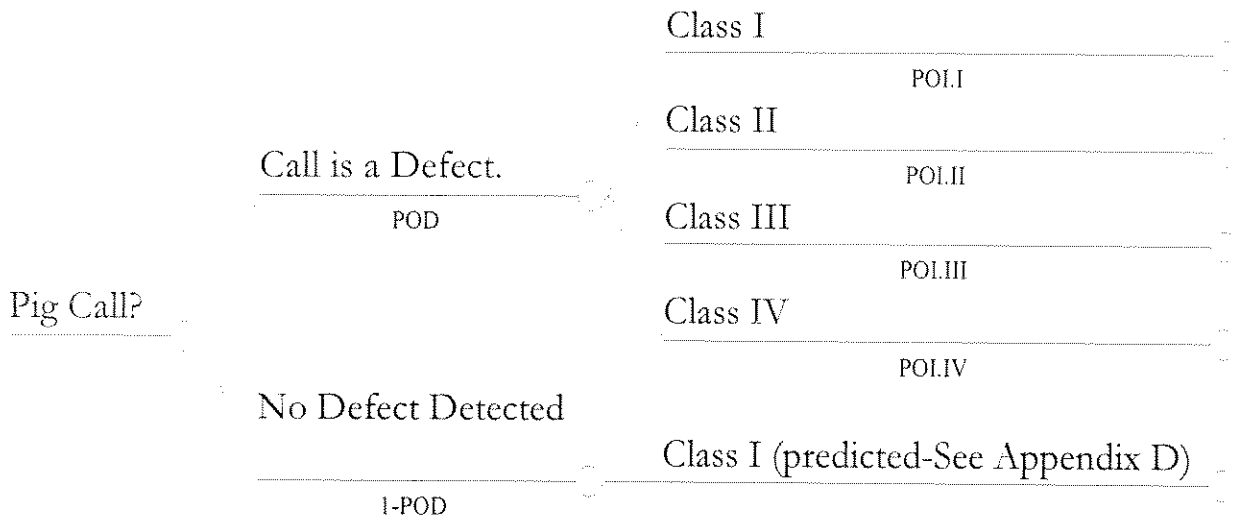

Figure 2.4.2: Actual Decision Tree

3. Summary of Current Pipeline Requalification Practice

3.1 ASME B31-G, 1991

The ASME B31-G manual is to be used for the purpose of providing guideline information to the pipeline designer/owner/operator with regard to the remaining strength of corroded pipelines. As stated in the ASME B31-G operating manual, there are several limitations to ASME B31-G, including:

- The pipeline steels must be classified as carbon steels or high strength low alloy steels;
- The manual applies only to defects in the body of the pipeline which have smooth contours and cause low stress concentration;
- The procedure should not be used to evaluate the remaining strength of corroded girth or longitudinal welds or related heat affected zones, defects caused by mechanical damage, such as gouges and grooves, and defects introduced during pipe or plate manufacture;
- The criteria for corroded pipe to remain in-service are based on the ability of the pipe to maintain structural integrity under internal pressure; and
- The manual does not predict leaks or rupture failures. (ASME, 1991)

The 'safe' maximum pressure (P') for the corroded area is defined as:

$$P' = 1.1P\left[\frac{1-\frac{2}{3}\left(\frac{d}{t}\right)}{1-\frac{2}{3}\left(\frac{d}{t\sqrt{A^2+1}}\right)}\right] \qquad \text{for } A = .893\left(\frac{Lm}{\sqrt{Dt}}\right) \leq 4$$

Where:
Lm = measured longitudinal extent of the corroded area, inches
D = nominal outside diameter of the pipe, inches
t = nominal wall thickness of the pipe, inches
d = measured depth of the corroded area
P = the greater of either the established MAOP of P = SMYS*2t*F/D
(F is the design factor, usually equal to .72)

3.2 Det Norske Veritas (DNV) RP-F101, Corroded Pipelines, 1999

DNV RP-F101 provides recommended practice for assessing pipelines containing corrosion. Recommendations are given for assessing corrosion defects subjected to internal pressure loading and internal pressure loading combining with longitudinal compressive stresses.

DNV RP-F101 allows for a range of defects to be assessed, including:

- Internal corrosion in the base material;
- External corrosion in the base material;
- Corrosion in seam welds;
- Corrosion in girth welds;
- Colonies of interacting corrosion defects; and
- Metal loss due to grind repairs.

Exclusions to DNV RP-F101 include:

- Materials other than carbon linepipe steel;
- Linepipe grades in excess of X80;
- Cyclic loading;
- Sharp defects (cracks);
- Combined corrosion and cracking;
- Combined corrosion and mechanical damage;
- Metal loss defects due to mechanical damage (gouges);
- Fabrication defects in welds; and
- Defect depths greater than 85% of the original wall thickness.

DNV RP-F101 has several defect assessment equations. The majority of the equations use partial safety factors that are based on code calibration and are defined for three different reliability levels. The partial safety factors account for uncertainties in pressure, material properties, quality, tolerances in the pipe manufacturing process and the sizing accuracy of the corrosion defect. The three reliability levels are: (1) safety class normal defined as oil and gas pipelines isolated from human activity; (2) safety class high defined as risers and parts of the pipelines close to platforms or in areas with frequent activity; and (3) safety class low defined as water pipelines.

There are several assessment equations that give an allowable corroded pipe pressure. Equation 3.2 gives P' for longitudinal corrosion defect, internal pressure only. Equation 3.3 gives P' for longitudinal corrosion defect, internal pressure and superimposed longitudinal compressive stresses. Equation 3.4 gives a P' for circumferential corrosion defects, internal pressure and superimposed longitudinal compressive stresses. Section Four of the manual provides assessments for interacting defects. Section Five assesses defects of complex shape.

It is important to note that the DNV RP-F101 guidelines are based on a database of more than seventy burst tests on pipes containing *machined* corrosion defects and a database of linepipe material properties. (DNV, 1999)

3.3 RAM PIPE Formulation (U.C. Berkeley)

RAM PIPE developed a burst equation for a corroded pipeline as:

$$P_{bd} = \frac{3.2 \cdot t_{nom} \cdot SMYS}{D_o \cdot SCF_C} = \frac{2.4 \cdot t_{nom} \cdot SMTS}{D_o \cdot SCF_C}$$

Where:

t_{nom} = nominal pipe wall thickness

D_o = mean pipeline diameter (D-t)

SMYS = Specified Minimum Yield Strength of pipeline steel

SCF_C = Stress Concentration Factor for corrosion features, defined by:

$$SCF_C = 1 + 2 \cdot (d / R)^5$$

The stress concentration factor is the ratio of maximum hoop stress over nominal hoop stress due to a notch of depth d in the pipeline cross section that has a mean radius R=(.5*D-.5*t)

(Bea, Xu, 1999)

4. RAM Background

4.1 Reliability and Quality

Reliability (Ps) is the likelihood or probability that the structure system will perform acceptability. The probability of failure (Pf) is the likelihood that the structure system will not perform acceptably (Pf = 1 – Ps).
Reliability can be characterized with demands (S) and capacities (R). When the demand exceeds the capacity, then the structure system fails. The demands and capacities can be variable and uncertain.
Quality is defined as freedom from unanticipated defects. Quality is fitness for purpose. Quality is meeting the requirements of those who won, operate, design, construct, and regulate structure systems. These requirements include those of serviceability, safety, compatibility, and durability.

(1) Serviceability is suitability for the proposed purposes, i.e. functionality. Serviceability is intended to guarantee the use of the structure system for the agreed purpose and under the agreed conditions of use.

(2) Safety is the freedom from excessive danger to human life, the environment, and property damage. Safety is the state of being free of undesirable and hazardous situations.

(3) Compatibility is also the ability of the structure system to meet economic, time, and aesthetic requirements.

(4) Durability assures that serviceability, safety, and environmental compatibility are maintained during the intended life of the structure system. Durability is freedom from unanticipated maintenance problems and costs.

4.2 Probability of Success and Failure

The probability or likelihood that the structure system will survive the demand is defined as the reliability:

$$Ps = P\,(R > S)$$

where P is read as the probability that the capacity (R) exceeds the demand (S). Ps is the probability of success, or reliability.
The probability of failure (Pf) is the compliment of the reliability:

$$Pf = 1 - Ps \text{ or } Pf = P\,(R < S)$$

The probability of failure can be occurred in any four-quality attributes of the system to lead the system to fail.

The cumulative probability distribution function for the resistance can be expressed as:

$$F_R\,(s) = P\,(R < s)$$

where $F_R\,(s)$ is read as the probability that the resistance, R, is equal to or less than a given value of the demand, s.
The probability density function for the loading can be expressed as:

$$fs\,(S) = p\,(s < S < s + \Delta s)$$

where p (S) is read as the probability that the loading is a particular value, S, in the interval from s to $s + \Delta s$.
Then, assuming independent demands and capacities:

$$Pf = \Sigma\, F_R\,[s]\; fs\,[S]\; \Delta s$$

In analytical terms, the reliability can be computed from:

$$Ps = \Phi\,(\beta)$$

where $\Phi\,(\beta)$ is the standard Normal distribution cumulative probability of the variants, β. β is commonly termed the Safety Index.

Given Lognormally distributed (these terms refer to the analytical model that describe the probability distribution of the parameter) independent demands (S) and capacities (R), β is computed as follows:

$$\beta = \frac{\ln(\underline{R}/\underline{S})}{\sqrt{\sigma_{\ln R}^{\,2} + \sigma_{\ln S}^{\,2}}} \text{ or } \frac{\ln(\underline{R}/\underline{S})}{\sqrt{\sigma_{\ln RS}^{\,2}}}$$

Given Normally distributed independent demands and capacities, β is computed as follows:

$$\beta = \frac{\ln(R - S)}{\sqrt{\sigma_R^{\,2} + \sigma_S^{\,2}}}$$

4.3 Central Tendency and Variability Measures

$\underline{R}$ and **R** are the median and mean capacities of the structure system, respectively. $\underline{S}$ and **S**

are the median and mean demands in the structure system, respectively.

The mean of a variable, **X**, can be computed from n values of the variable, X, as follows:

$$\mathbf{X} = \Sigma \frac{X}{n}$$

For Normally distributed variables, the mean, mode, and median are all the same values (symmetrical distribution). For Lognormally, distributed variables, the mean, mode, and median generally are all different values. A Lognormal distribution is a Normal distribution of the logarithms of a variable.
A Normal distribution will result from the addition of a large number of random variables. A Lognormal distribution will result from the multiplication of a large number of random variables.
In the case of Lognormally distributed variables, the mean, **X**, is related to the median, $\underline{X}$, by:

$$\mathbf{X} = \underline{X} \exp (0.5\ \sigma_{\ln X}^2)$$

where $\sigma_{\ln R}$ is the standard deviation of the logarithm of the capacities. $\sigma_{\ln S}$ is the standard deviation of the logarithm of the demands. $\sigma_{\ln RS}$ is the standard deviation of the logarithms of the demands and capacities.

Coefficient of variation for Lognormal distribution, Vx, can be expressed as follows:

$$\sigma_{\ln X} = \sqrt{\ln(1 + Vx^2)} \text{ or } Vx = \sqrt{\exp^{\sigma \ln x^2} - 1}$$

$$\text{For } Vx < 0.3,\ \sigma_{\ln x} \cong Vx$$

4.4 Uncertainties

Uncertainties associated with structure loadings and capacities will be organized in two categories. The first category of uncertainty is identified as natural or inherent randomness (Type I uncertainty). Example of Type I uncertainty associated with loadings are the annual maximum wave height, earthquake ground acceleration, or ice impact kinetic energy that will be experienced by a structure at a given location during a given period of time in the future. Examples of Type I uncertainty associated with capacities are the yield strengths of steel, tensile strength of copper, and shear strength of any material.
A second category of uncertainty is identified as unnatural, cognitive, parameter, measurement, or modeling uncertainty (Type II uncertainty). This type of uncertainty applies to deterministic, but unknown value of parameters; to modeling uncertainty; and to the actual state of the system. Example of Type II uncertainty in loadings are the uncertainties in computed wind, wave and current, earthquake, and ice conditions and forces that are due to imperfections in analytical models. Examples of Type II uncertainty in capacities is the difference between the nominal yield strength of steel and the mean or

median yield strength of the steel, and between the true buckling capacity of a column and that determined from an Euler buckling column formulation.
In this development, Type I uncertainty is characterized with two parameters:

(1) Central tendency measures of the parameter of concern, X (median, $\underline{X}$, and mean **X**) and
(2) Dispersion measure of X, (coefficient of variation, Vx, standard deviation, σ_x)

Type II uncertainty is characterized with two parameters:

(1) Central tendency measures of the Bias, B (median, $\underline{B}$, mean, **B**) and,
(2) Dispersion measure of the Bias, the coefficient of variation, V_B

Bias is defined as the ratio of the true or actual value of a parameter to the predicted (design, nominal) value of the parameter:

$$B = \frac{\text{True or Measured Value}}{\text{Predcited or Nominal Value}}$$

4.5 Time Considerations

The time period that often is used to define the probability characteristics of the loadings and capacities is one year. If the capacity were changing as a function of time, for example, due to fatigue degradation of the strength, then Pf could be determined for discrete time intervals recognizing the change in the capacity, and the Pf is summed over the total exposure period (L).
Relating the annual risk, Pf_a, to the lifetime risk, Pf_L, is simple if each year is considered a statistically independent event (no correlation of trials from year to year). In this case, for a lifetime of L years:

$$Pf_L = 1 - (1 - Pf_a)^L$$

For small Pf_a, this gives:

$$Pf_L = L\, Pf_a$$

However, there is correlation of risk from year to year due to statistical dependence through several important variables in Pf including the structure resistance, some of its loadings (e.g. dead loadings), and some of the sources of uncertainty (e.g. methods of analysis). Many of the variables are independent of the natural randomness associated with such occurrences as storms or earthquakes, and may be considered constant during the lifetime. If one takes the other extreme assumption, and considers perfect dependence or correlation from year to year, then:

$$Pf_L = Pf_a$$

4.6 Evaluation of Variability and Correlations

To evaluate the variabilities of the demands and capacities from the components of the demands and capacities that contribute uncertainties, one can use the algebra of Normal Functions. This approach is equivalent to a first order – second moment (FOSM) method to propagate the central tendencies and uncertainties of multiple parameters. This approach is based on a first order Taylor Series expansion of the distribution characteristics and then retention of only the first two terms of the expansion.
For the addition or subtraction of two random variables, $(X \pm Y) = z$, the mean (same as mode and median) of the resultant distribution can be calculated as follows:

$$Z = X + Y$$

The standard deviation of the resultant distribution can be calculated as follows:

$$\sigma_Z = \sqrt{\sigma_X{}^2 + \sigma_Y{}^2 \pm 2\rho\sigma_X\sigma_Y}$$

ρ is the correlation coefficient between the two variables X and Y.

For the multiplication of two random variables, $(XY) = Z$, the mean of the resultant distribution can be calculated as follows:

$$Z = XY + \rho\,\sigma_X\sigma_Y$$

The standard deviation of the resultant distribution can be calculated as follows:

$$\sigma_Z = XY\sqrt{(1+\rho^2)[V_X{}^2 + V_Y^2 + (V_X^2 V_Y^2)}$$

When the random variable X and Y can be considered independent ($\rho = 0$), and V_X and V_Y are small ($V \ll 1$), then:

$$V_Z \cong \sqrt{V_X^2 + V_Y^2}$$

For the division of two random variables, $(X/Y) = Z$, the mean of the resultant distribution can be calculated as follows:

$$Z = X/Y$$

The standard deviation of the resultant distribution can be calculated as follows:

$$\sigma_Z = (X/Y)\sqrt{V_X{}^2 + V_Y^2 - 2\rho(V_X V_Y)}$$

When the random variable X and Y can be considered independent ($\rho = 0$), and Vx and V_Y are small (V<<1), then:

$$Vz \cong \sqrt{V_X^2 + V_Y^2}$$

To determine the product of two variables when one of the variables is raised to a power ε ($Z = XY^{\varepsilon}$):

$$Z = X\,(Y)^{\varepsilon} + \rho\,\sigma_X\sigma_Y$$

and

$$\sigma_Z = X(Y)^{\varepsilon}\sqrt{(1+\rho^2)[V_X{}^2 + V_Y^2 + (V_X^2 V_Y^2)}$$

When the random variable X and Y can be considered independent ($\rho = 0$), and Vx and V_Y are small (V<<1), then:

$$Vz \cong \sqrt{V_X^2 + (\varepsilon V_Y)^2}$$

The correlation coefficient, ρ, expresses how strongly two variables, X and Y, are related to each other. It measures the strength of association between the magnitudes of two variables. The correlation coefficient ranges between positive and negative unity ($-1 \leq \rho \leq 1$).

If $\rho = 1$, they are perfectly correlated, so that knowing X allows one to make perfect predictions of Y. If $\rho = 0$, they have no correlation, or are independent, so that the occurrence of X has no affects on the occurrence of Y and the magnitude of X is not related to the magnitude of Y.

The correlation coefficient can be computed from data in which the results of n samples of X and Y are developed:

$$\rho = \frac{\sum XY - nXY}{\sqrt{(\sum X2 - nX2)(\sum Y2 - nY2)}}$$

There can be correlations between demands and capacities. As the demands changes, the capacities can change. Increasing loadings resulting in decreasing capacities are an example of negative correlation in the demand and capacity.

Fro the case of Lognormally distributed correlated demands and capacities, β is computed as follows:

$$\beta = \frac{\ln(\underline{R}/\underline{S})}{\sqrt{\sigma_{\ln R}{}^2 + \sigma_{\ln S}{}^2 - 2\rho\sigma_{\ln R}\sigma_{\ln S}}}$$

B) POD estimation approaches from two different industries and Qualitative description of POD for MLF

1. Modeling POD: Qualitative analysis from the aerospace industry

1.1 Benefits of modeling POD

Aside with the experimental approach for getting POD, modeling is developing to become a useful approach for POD estimation.
The advantage of using models is that parametric studies of performance can be made with relative ease and little expense. Typically, work would be performed that varied a parameter (such as scan rate, defect orientation, threshold setting) to obtain consistent estimates of their effect on POD and PFI. This then allows a considered optimization of the inspection to be performed with regard to costs and benefits. A second very important advantage of model calculations is that there are very little experimental data on false-calls PFI and the model is usually the only source of data for them. Modeling also allows assessment of historical data, optimization at the design stage and allows valuable experimental data to be extended to new applications. Given the poor statistics and large scatter in many POD trials it is arguable whether these provide more accurate values than a modeling or simulation approach.

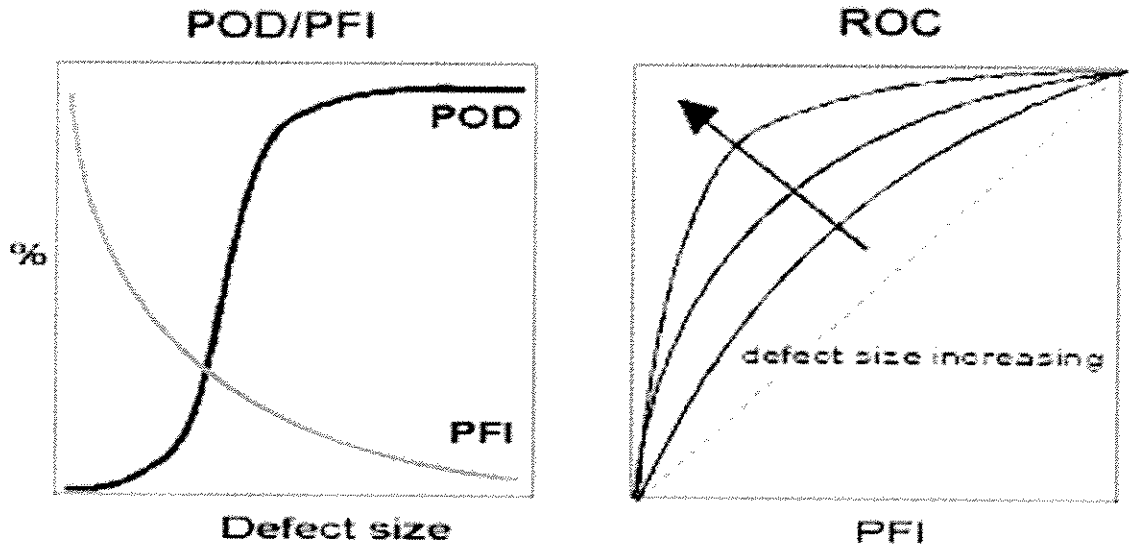

Fig 1.1: Defect size POD and PIF curves

1.2 Approaches to modeling of POD

There are many established models for inspection techniques which can estimate the signal associated with individual defects in a component, for example AEA Technology's ultrasonic ray tracing model RAYTRAIM. It is only recently that models have evolved which include the additional factors (noise, geometry, defect visibility and human factors) needed to make effective predictions of POD. The approaches presently available to make predictions of POD take one of several forms and can be summarized as follows:

- Physical models for POD and PFI
- Signal/Noise models
- Image classification models/ Inspection simulators ('Visual' POD, 'Spot the Ball')
- Expert judgment
- Statistical models (Curve-fitting)
- Human reliability models

1.3 Current status

1.3.1 Physical POD Models

Physical models for POD and PFI provide data through a physical model of the inspection process, including background noise and criteria for defect detection. During the last 5 years a suite of models has been developed within the National NDT Center for predicting inspection reliability in terms of probability of detection POD and false calls (PFI). These models use established and well-validated physical models as their basis but also include variable factors such as noise, geometry, and defect visibility and detection criteria necessary to make predictions in reliability terms. All models run on a standard PC in real time and cover a range of inspection methods including ultrasonic (pulse-echo and time-of-flight), radiography and magnetic techniques. Customized models have been developed for specific applications including validation of a procedure for detection of complex weld defects, inspection of steel railway line, composite materials, and inspection of concrete structures. The models allow analysis of image-based data, produce simulated images and allow correction for human and environmental effects. The estimates of POD combine estimates of signals expected from specific defects and transducers, estimates of background noise and a 'threshold criterion'. The simulation of defects is being constantly improved based on the analysis of 'real defect' data from operating plant.

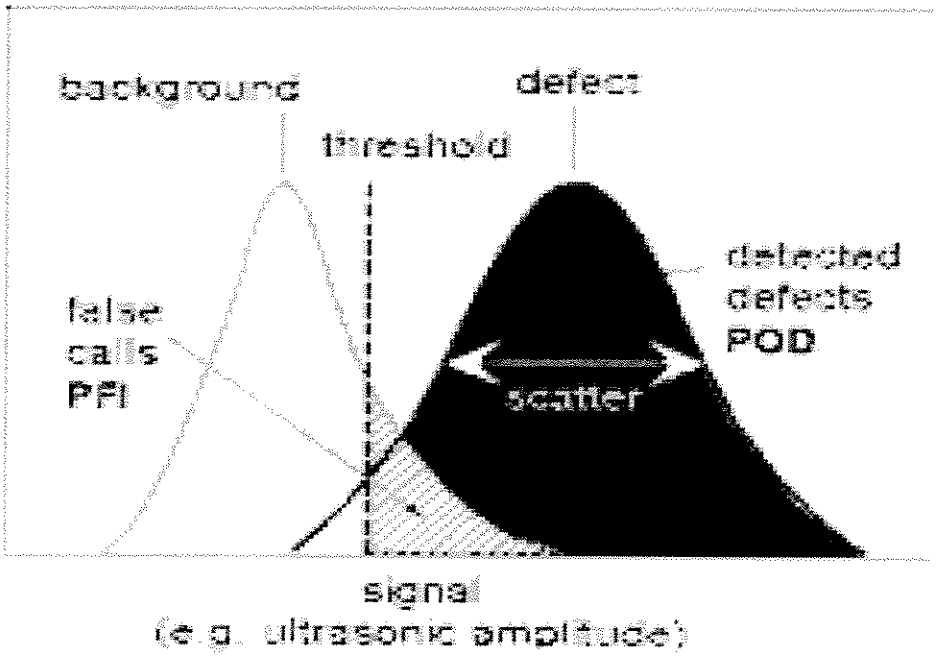

Fig 1.3.1: Probabilistic explanations of PFI and POD

1.3.2 Signal/Noise models

These convert signal and noise values to POD and PFI using statistical methods. The signal and noise values can be derived from models or experiment, for example measurements on samples with reference defects. The approach in calculating POD is similar to the physical models above. This method avoids the statistical difficulties associated with conventional POD trials and allows predictions to be made for new inspection techniques that may be too complex to physically model. This approach has been used for many years in the USA aerospace industry. A modular approach can be adopted, with input data to the POD model derived from a physical model or experiment..

1.3.3 Image classification models/ Inspection

These represent methods for analysis of image-based inspection data such as radiographs, to give information in terms of POD and PFI. Inspection simulators are a special class of computer model that simulates the inspection process by presenting simulated inspection results to the operator. Interpretation of image-based data is more difficult and requires a more complex detection criteria than analysis of signal/noise data above. The detection criterion may be simply exceeding a threshold signal level at a number of locations, over a number of pixels or over a specified area or more closely configured to actual inspection system operation. There is now a neural-network based approach for detection of defects in image-based technique. This uses receptive fields to search for and enhance

specific defect types such as cracks porosity or slag inclusions and more closely reproduces the human interpretative skills of the inspector.

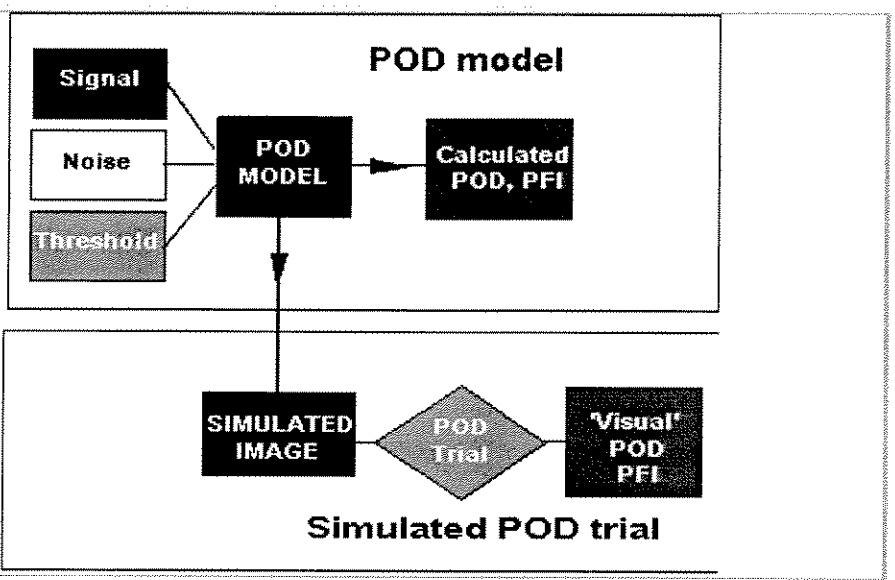

Figure 1.3.2 : Schematic illustrating the basis of a POD model and the use of simulated images for POD trials to aid in the validation of model predictions. ('Visual POD', 'Spot-the-ball contest').

The production of simulated images and inspection data is an important feature in POD models. The images give confidence that the simulation and POD estimates are reasonable. The programmers can present a series of simulated images to the inspector like a 'spot the ball' contest, essentially simulating a POD trial (Figure 1.3.3). The POD and PFI is automatically calculated, we call this 'Visual POD'. This provides a second independent method for the model to estimate POD and comparison can provide information on human reliability. A similar simulation method was used in the PISC III program on human reliability.

1.3.4 Expert Judgment

Expert judgment has been used where input on POD is required for fracture mechanics or risk-based assessments and is not available from experiment. Provided the judgment comes from trained inspectors and sensitivity analysis is used this can be an effective method. The National NDT Center maintains a computer database of POD information (PODDATA), which can be used to aid such judgments.

1.3.5 Statistical models

These use methods for statistical analysis or curve fitting to experimental data, with the aim of making this data accessible for use in other applications (such as fracture mechanics). These do not model the inspection process as such.

1.3.6 Human reliability models

These take account of the effects of human error in the inspection process, and correct predicted POD values for these effects. An example is the methodology applied by AEA Technology to utilize human error data from the PISC III work discussed later.

1.3.7 POD Models for Aerospace

A major POD modeling contract is underway by AEA Technology, National NDT Center for the European Space Agency ESA (ESTEC Contract 12228/96). This commenced in February 1997 and has 20 Month duration. Models are being developed to predict POD and PFI for composite aerospace components and validated by experimental trials. Two specific NDT techniques are included: ultrasonic C-scan and X-radiography. In addition a 'technique-independent' model, based on the signal/noise approach above, will allow POD predictions to be made from image-based or signal-noise data for evolving techniques such as transient thermography. All models will produce simulated images, which can be used in place of real samples for POD trials and provide an independent route ('Visual POD) for verification of the model POD predictions. It is anticipated the models will lead to improvements in the quality and understanding of aerospace NDT and could be adapted to other materials and structures.

1.3.8 Examples of Model Application: Parametric Studies

The specific application of a POD model to examine the effect of a single parameter is illustrated in Figure 1.4.1. This shows the effect on POD for ultrasonic inspection of defect orientation; allowing a crack to be mis-orientated by up to +/-15. Such data would be complex to determine by experiment. Figure 2.5.5 shows the effects of varying inspection threshold and defect size on the POD for radiographic inspection calculated using model XPOSE, in this case plotted in terms of an ROC curve. Figure 6 shows an example-simulated radiograph and corresponding predicted POD and PFI curves. XPOSE sets up the inspection in the same way as a radiographer, and then produces simulated radiographs as well as POD and PFI predictions. The resulting POD values may be compared to the visual perception of the defect in the radiograph. Standard defects include voids, porosity, inclusions, lack of fusion defects and cracks. The simulated radiograph also shows the series of Image Quality Indicator (IQI) lines used as reference in the inspection as in routine radiographic work.

1.4 Examples of Model Application

1.4.1 Parametric Studies

The specific application of a POD model to examine the effect of a single parameter is illustrated in Figure 1.4.1 .
This shows the effect on POD for ultrasonic inspection of defect orientation; allowing a crack to be mis-orientated by up to +/-15 (. Such data would be complex to determine by experiment. Figure 1.4.2. shows the effects of varying inspection threshold and defect size on the POD for radiographic inspection calculated using a model, in this case plotted in terms of an ROC curve. Figure 1.4.3 shows an example-simulated radiograph and corresponding predicted POD and PFI curves. The model sets up the inspection in the same way as a radiographer, and then produces simulated radiographs as well as POD and PFI predictions. The resulting POD values may be compared to the visual perception of the defect in the radiograph. Standard defects include voids, porosity, inclusions, lack of fusion defects and cracks. The simulated radiograph also shows the series of Image Quality Indicator (IQI) lines used as reference in the inspection as in routine radiographic work.

1.4.2 Comparison of Techniques

Figure 1.4.1. consider inspection for a surface crack-like defect in 25mm steel plate mis-orientated by up to 10 (and compares the use of time-of-flight diffraction (TOFD), pulse-echo ultrasonic and radiography. As the defect is tilted away from normal radiography and conventional UT become progressively less suited, whereas TOFD, which is dependent on diffraction from the defect tips, remains effective. This is illustrated by the calculated POD's. These model predictions are almost identical to experimental POD.

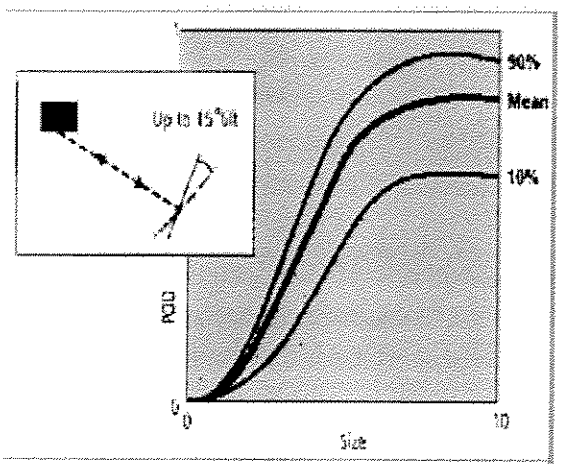

Figure 1.4.1: Effect of varying a single parameter: defect tilt.POD model calculations using PODUT

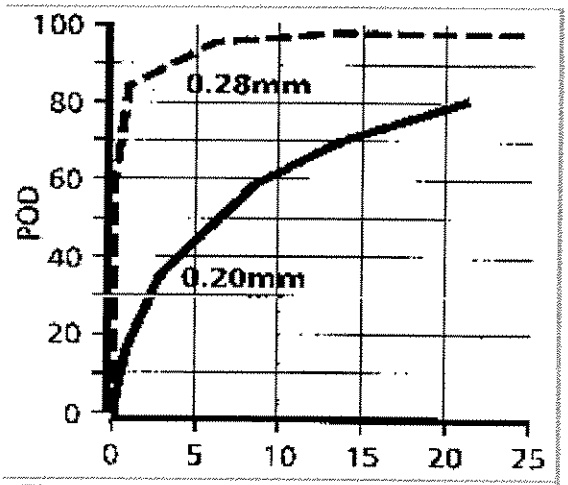

Figure 1.4.2: Model predictions of POD,PFI and ROC for voids in steel plate using radiographic POD model XPOSE. The detection threshold is varied

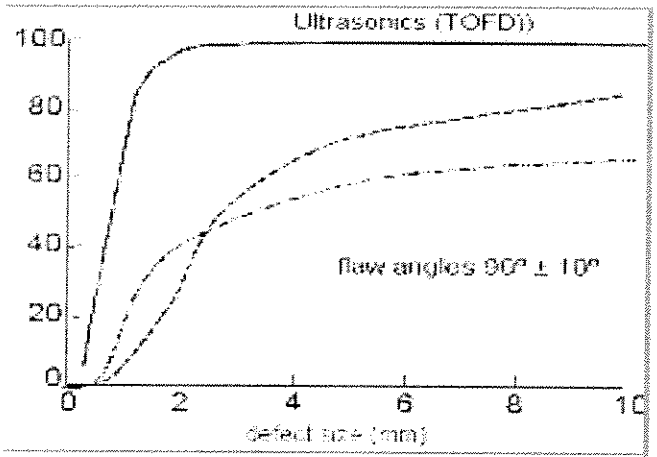

Figure 1.4.3: Comparison of techniques: POD model calculations for inspection for mis-orientated cracks in 25mm plate.

1.5 Correction for Human Factors

Inspection reliability is clearly quite complex to model and must include consideration of procedure, material, human and environmental factors. Human factors have recently been shown to be very important and dependent on a large number of factors such as fatigue, environment, stress and complexity of the task. We distinguish between tasks involving the 'eye' and ' hand-eye coordination'. It is unlikely that a theoretical model of this will be developed in the near future. However, experimental data is being amassed in a number of fields including NDT. The physical models described above give a 'theoretical' or 'physically achievable' POD, allowing variation in parameters such as defect orientation

or visibility. In order to give model predictions comparable to those that would be found in experimental trials we use a human factor curve as a multiplier H for models based on the physics and engineering of an inspection.

$$PODactual = POD\ model * H$$

The simplest correction uses a constant multiplier (or POD reduction factor), typically 95% or lower for more severe environments. A better correction method uses curves such as the data for human error expressed in terms of POD in Figure 1.4.3. This recognizes that the effects of human error are greater for small defects close to threshold. In this case the human error POD is used as the multiplier H.

A general equation was suggested in which the theoretical POD was reduced to take account of environmental effects:

$$POD\ actual = POD\ intrinsic - g(AP) - h(HF)$$

Where g(AP) and h(HF) are factors relating to the application of the technique (environment, surface, couplant, geometry etc.) and human error respectively.

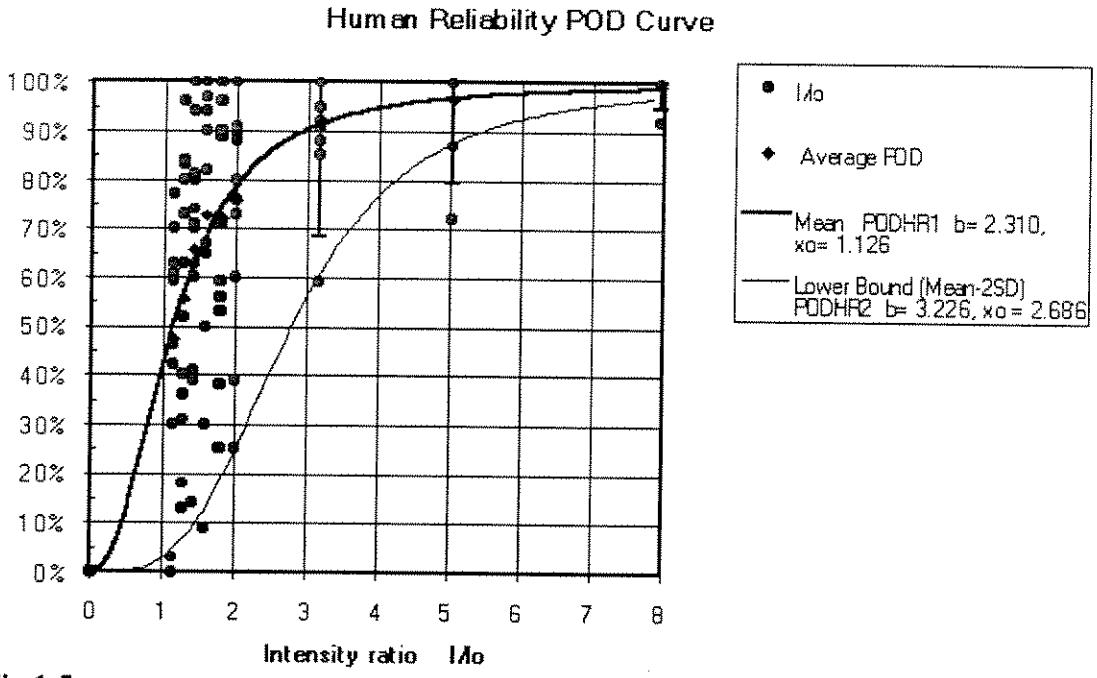

Fig 1.5

1.6 Validation

Validation of the models is important in gaining increased acceptance for their use. The validation needs should be considered in the context of the application. For example, in probabilistic fracture mechanics assessments or economic assessments sensitivity studies

are often included and therefore upper and lower bound data may be used in place of absolute values. Second, much scatter can arise in experimental POD trials: therefore model calculations only need to be similarly accurate to offer a realistic alternative. To validate existing POD models we have used the following approaches:

- Comparison with experimental POD data.
- Parametric studies
- Compare simulated images with actual images (e.g radiographs)
- Use simulated images in POD trials *('Visual POD')*.

Where comparison with experiment is possible, reasonable agreement has been found between model calculations and experiment and parametric variations observed in experimental data are reproduced by models. One such comparison is given in Figure 1.6 and for the TOFD model similar comparisons have been given. For precisely defined input data model POD curves are generally sharper than experiment, but more realistic curves are obtained if 'randomizing factors' such as defect orientation, background, attenuation or defect visibility are allowed to vary between practical limits found in real components.

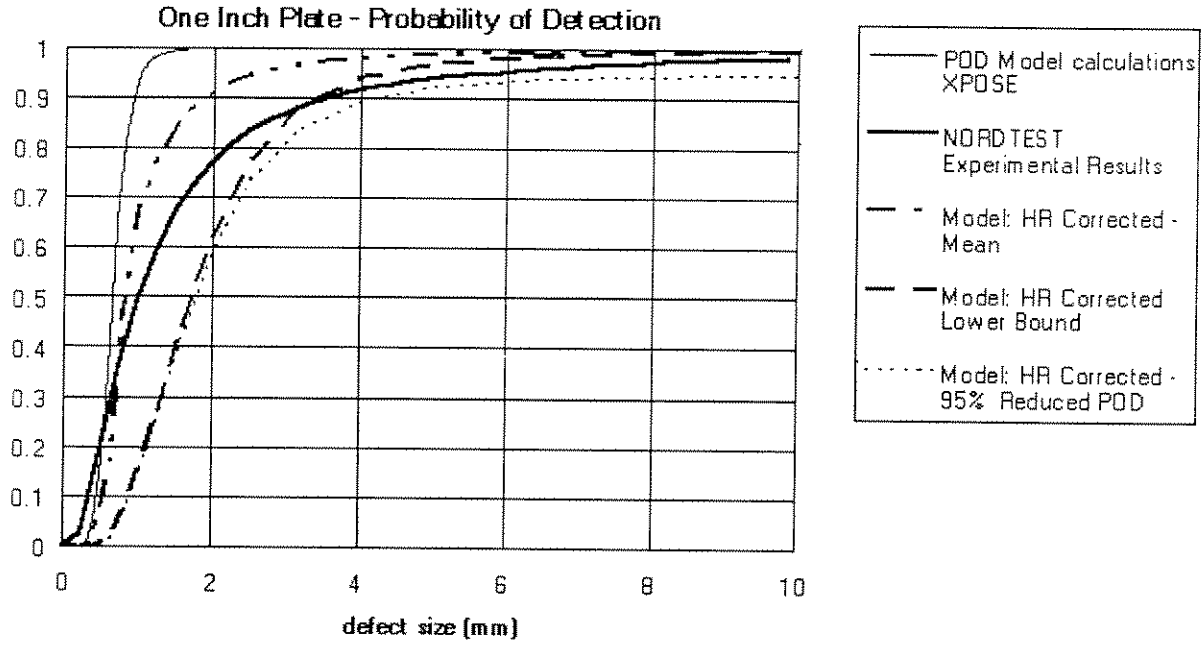

Fig 1.6

2. Insight on POD of radiographic inspection methods

2.1 The Task

It is the objectives of this study to develop acceptance criteria for the mechanized and automated ultrasonic pipeline girth weld examination systems (AUK) for use during pipeline construction to inspect the fabrication girth welds, and to document the adequacy of these acceptance criteria for the task in question. This is primarily done with respect to replacing the fabrication quality control radiography, which in this case represents the accepted concept. Later also the topic of fitness-for-purpose acceptance criteria will be addressed.
With respect to the replacement of radiography by AUK the following items are crucial

- AUK must do 'as good a job' as radiography in revealing significant defects
- AUK must not produce to many false calls, or lead to increase in repair rates, rather a lowering, in order to provide for cost-effectiveness
- The documentation of the AUK performance must, in order to be useful, have sufficient statistical confidence.

Nomenclature
The abbreviations used further below are:

RL: Ultrasonic reference level, corresponding to the echo from a 3 mm diameter side drilled hole
E: Ultrasonic echo amplitude
L: Measured defect length
h: TOFD measured defect height
t: Material thickness

2.2 Acceptance Criteria

In the examples shown slight modifications of the acceptance criteria of the DNV pipeline rules were used. In addition, acceptance criteria based on simulated TOFD measured heights[1] to replace the echo amplitude criteria of the DNV rules were applied. The applied rejection criteria, in a simplified version, are:

[1] Assuming no mean error in measurement and a standard deviation of 1.3 mm based on other research work.

Radiography	**Ultrasonics**[2]	Amplitude based	TOFD based
			E > RL- 12dB and
L > t, max.2 5mm	L < t/2:	E > RL+4dB	h > 4mm
L < t: IIW degree Red or Brown[2]	t/2 < L < t:	E > RL -2dB	h > 2mm
Evaluation as crack	L > t::	E > RL- 6 dB	h > 1 mm

[2] For surface defects. There are slightly other length criteria for embedded defects and thick plate (> 25 mrn thickness).

[3] Reflecting also the rejection of spherical cavities or inclusions of 3 mm diameter or more.

2.3 Probability of Detection Curves

To describe the ability of an NDE (non-destructive examination) technique to reveal defects, POD[4] curves, or POD values for groups of defects, can be used and compared utilizing the Elementary Detection Criteria of the Nordtest comparison and replacement guidelines. The diagrams contain maximum likelihood regression POD curves (thick lines) with lower one-sided 95% confidence limit (thin lines), and for the reference radiography curve also the regression values minus 0.1 as used for the Nordtest criteria (thick chopped lines). All curves give POD as function of defect height, which is regarded the most predominant defect severity parameter.

[4] POD is here also used a synonym for Probability of Rejection: The NDE system Including the acceptance criteria used can be regarded a 'black box' either detecting a defect, or not.

2.4 Comments

Figs. 2.4.1. and 2.4.2. show grouped POD observation data with fitted curves. Fig 2.4.1. Contains all the radiographic data contained in the Nordtest Programme, whereas Fig. 2.4.2. only contains approximately 150 randomly selected observations. In the latter case, the lower 95% confidence limit is just above the fitted mean curve minus 0.1, and the NordtestElementary Detection Criteria still fulfilled for the Reference Technique. Fig.

2.4.2. thus gives an indication of the number of observations required to fulfill the criteria.

Figs. 2.4.3. And 2.4.4. Give comparative curves for a mixture of all encountered defect types and, the pipeline girth weld important defect type, lack of fusion. The echo amplitude criteria can be regarded satisfactory for all defect heights, whereas the TOFD acceptance criteria are satisfied according to the Nordtest requirements above defect height 2 mm, corresponding to the radiography 0.5 POD. This must also be regarded satisfactory. In addition, it can be noted that the TOFD curves are steeper than the echo amplitude based curves. This is of course due to the better correlation between TOFD measured defect height and true defect height, than between echo amplitude and height, and implies a better quality examination work with TOFD, as less small and more large defects are revealed (please keep though in mind that the TOFD POD data are a simulation). The total (small and large defects) detection / rejection rate for TOFD is 45% compared to 46% for radiography.

Fig. 2.4.5. Shows the inadequacy of the set acceptance criteria for ultrasonic for porosity. In order to reveal pores with ultrasound higher sensitivities than those used must be applied: At 30 mm distance a spherical cavity of 4 mm 0 gives an echo 11 dB below that of a 3 mm 0 side drilled hole, etc. One way to handle this problem is to do an evaluation of the severity of pores (and similar for slag inclusions), and possibly accept relaxed acceptance criteria compared to those for radiography, or use special ultrasonic pattern recognition techniques to map porosity.

Figs. 2.4.6. And 2.4.7. Compare POD curves for lack of fusion in different thickness groups (average wall thickness 13 and 28 mm), and show that the ultrasonic echo amplitude criteria are not adequate for the thinner material.

Fig. 2.4.8. Shows the failure of the set ultrasonic echo amplitude acceptance criteria for lack of fusion of less length than wall thickness. Some caution is, however, required, when making this observation: The used acceptance criteria for radiography allow lack of fusion of length below wall thickness, and the detections made are due either to misinterpretation of defect type or length, or the evaluation as IIW degrees Red or Brown incorporated in the acceptance criteria. There is, however, as further analysis shows, a POD defect length dependency, and an evaluation of this length dependency is required, when lengths are not 'naturally' distributed, or defect significance is also length dependent, as when plastic collapse is the most relevant defect mechanism related to the girth weld defects. Further, a distinction may have to be made between surface and embedded defects.

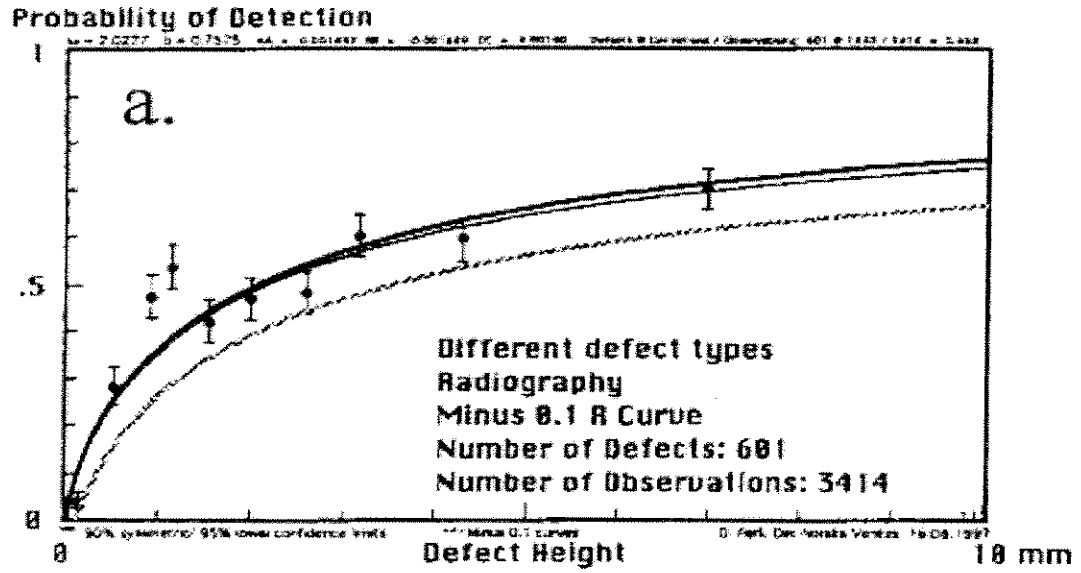

Figure 2.4.1: Different defect types Radiography Minus 0.1 R Curve Number of Defects: 601 Number of Observations: 3414

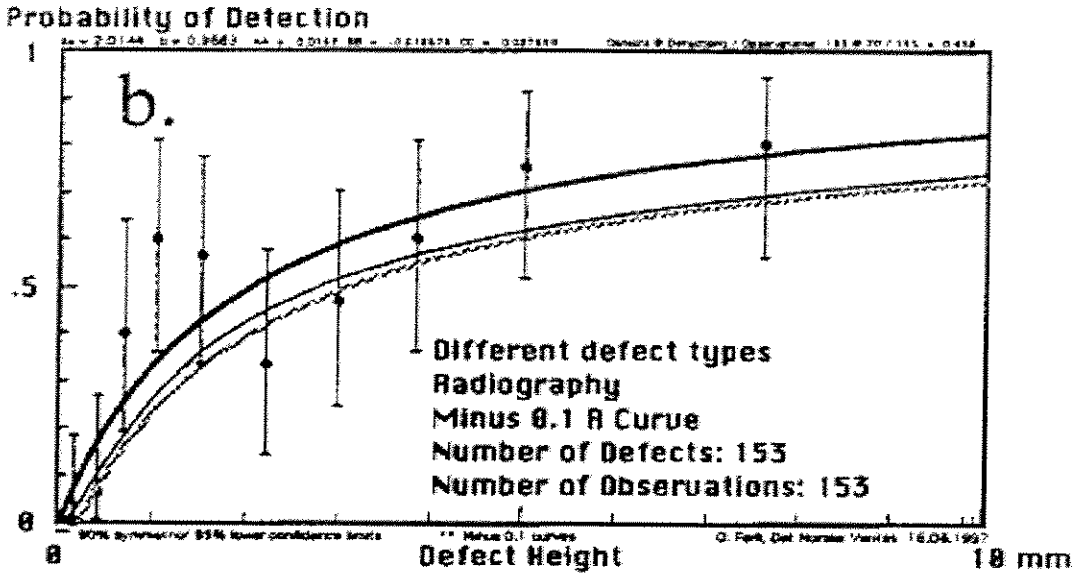

Figure 2.4.2: Different defect types Radiography Minus 0.1 R Curve Number of Defects: 153 Number of Observations: 3414

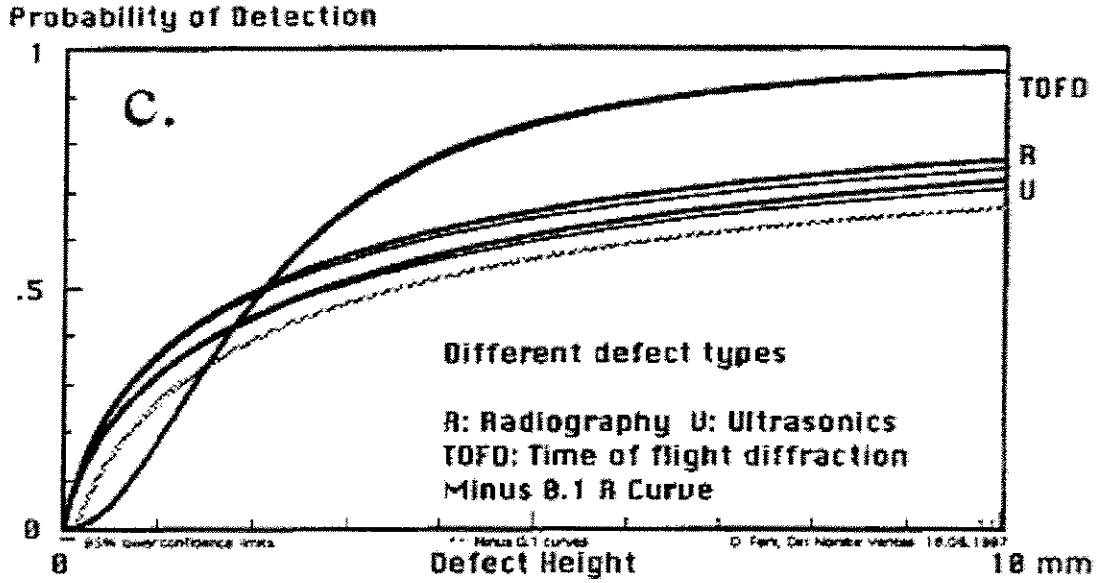

Figure 2.4.3: Different defect types R: Radiography U: Ultrasonic TOFD: Time of flight diffraction Minus 0.1 R Curve

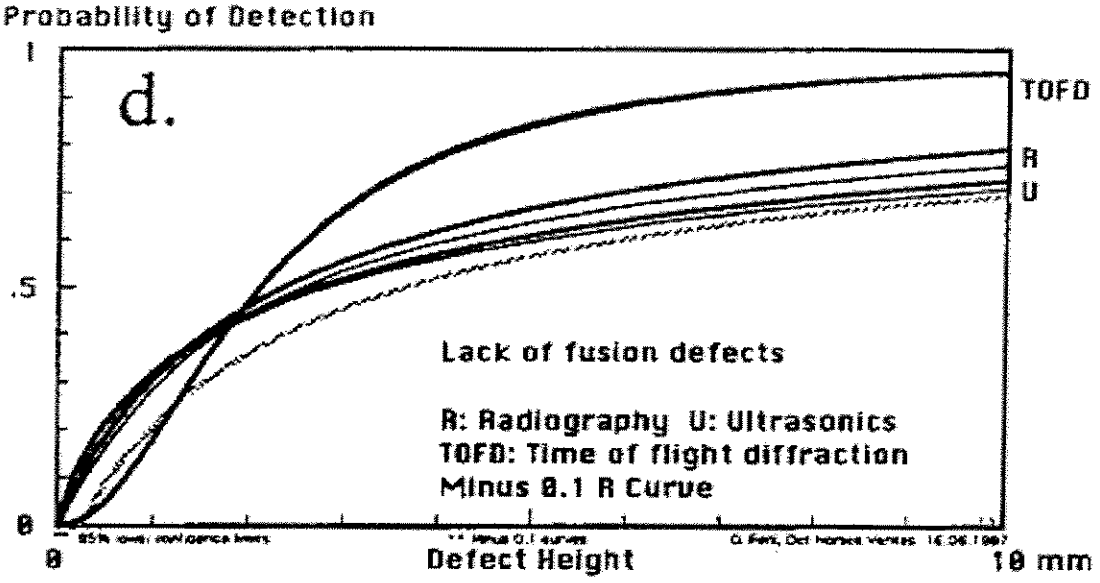

Figure 2.4.4: Lack of fusion defects R: Radiography U: Ultrasonic TOFD: Time of flight diffraction Minus 0.1 R Curve

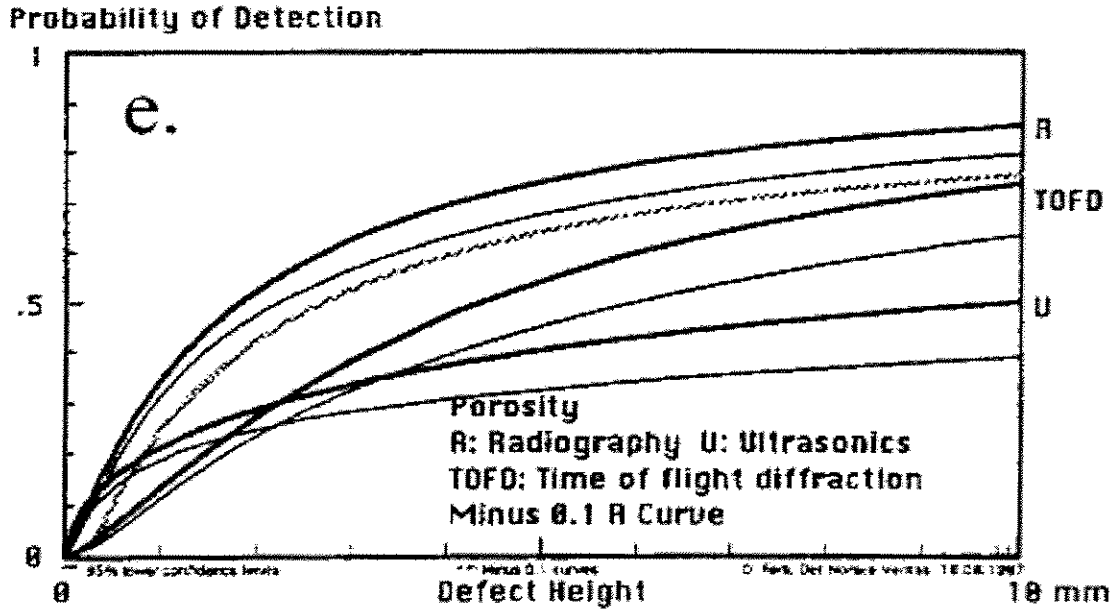

Figure 2.4.5: Porosity R: Radiography U: Ultrasonic TOFD: Time of flight diffraction Minus 0.1 R Curve

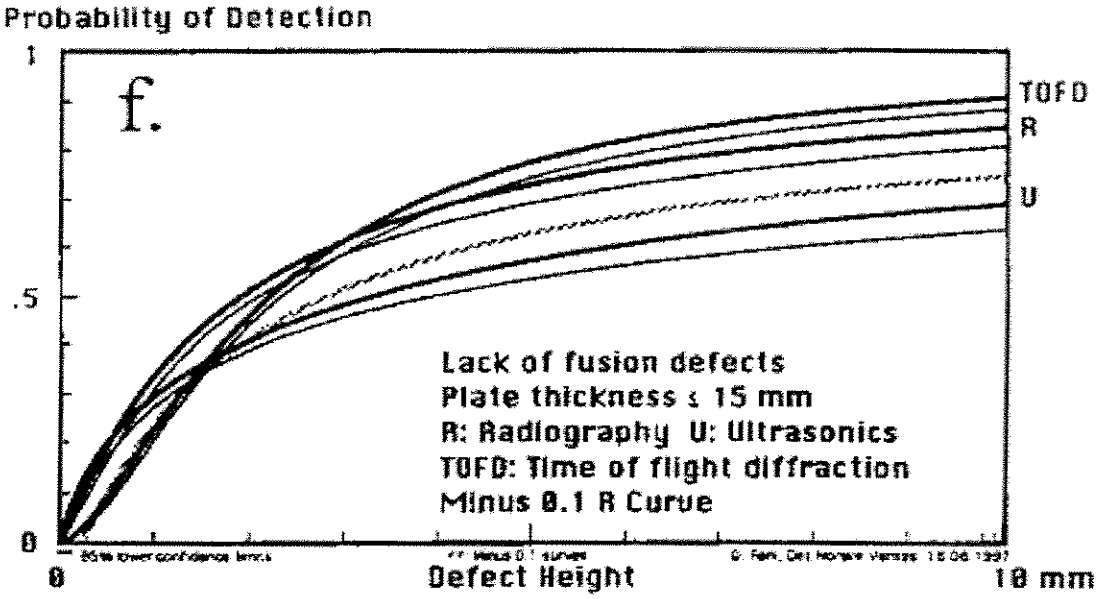

Figure 2.4.6: Lack of fusion defects Plate thickness < 15mm R: Radiography U: Ultrasonic TOFD: Time of flight diffraction Minus 0.1 R Curve

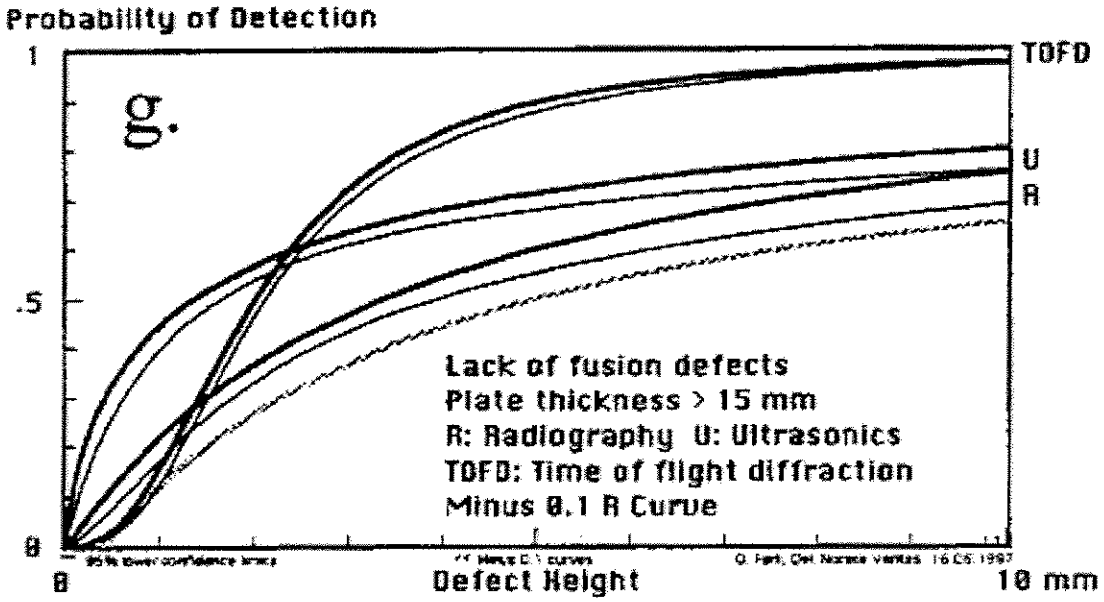

Figure 2.4.7: Lack of fusion defects Plate thickness > 15mm R: Radiography U: Ultrasonic TOFD: Time of flight diffraction Minus 0.1 R Curve

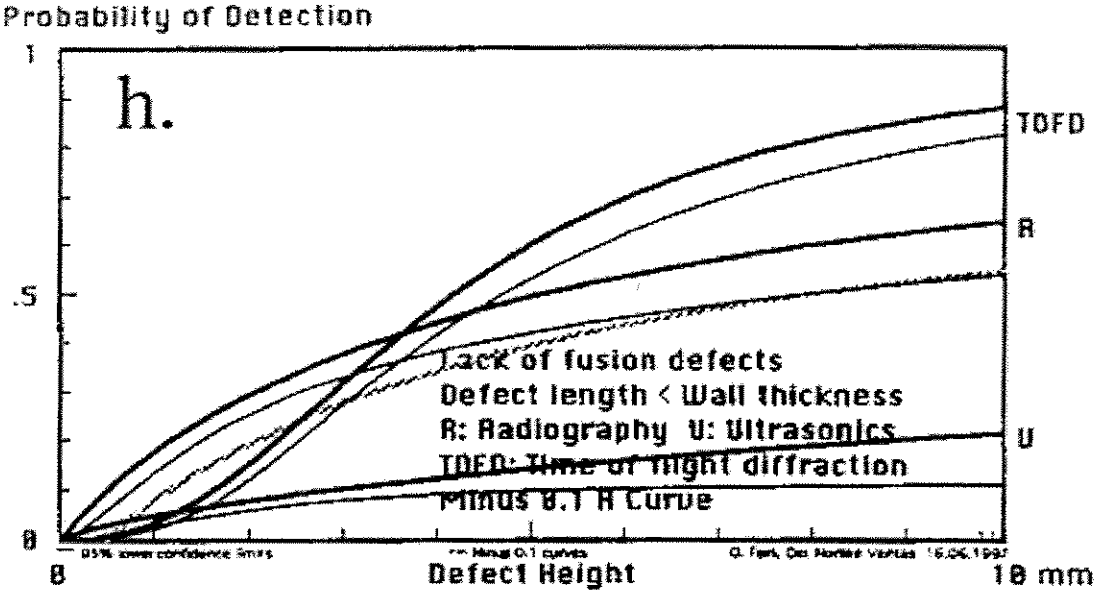

Figure 2.4.8: Lack of fusion defects Defect length < Wall thickness R: Radiography U: Ultrasonic TOFD: Time of flight diffraction Minus 0.1 R Curve

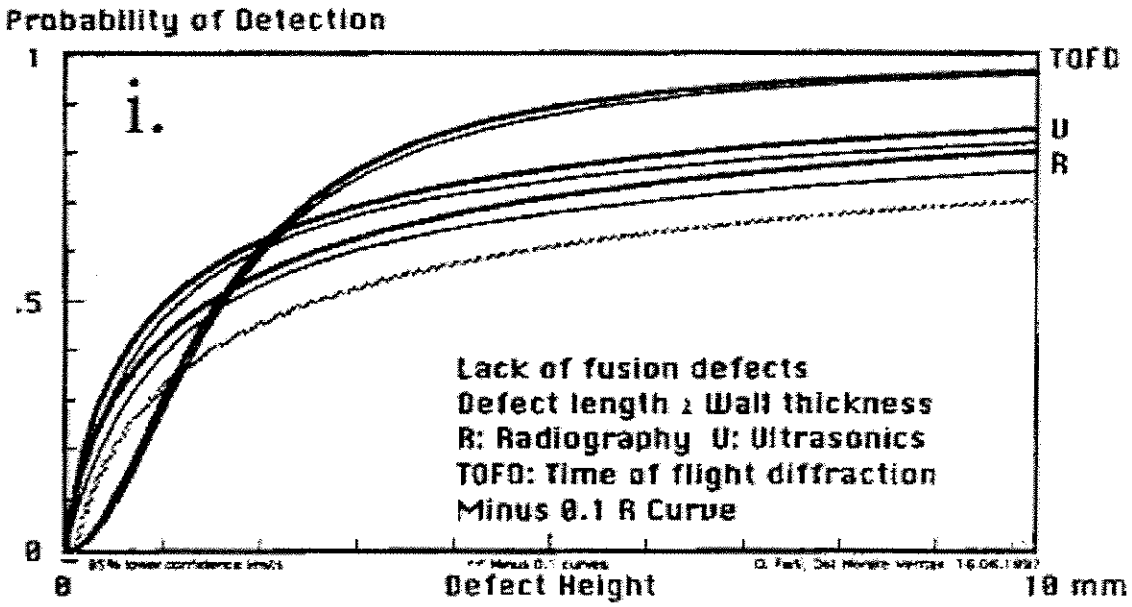

Figure 2.4.9: Lack of fusion defects Defect length > Wall thickness R: Radiography U: Ultrasonic TOFD: Time of flight diffraction Minus 0.1 R Curve

2.5 Fitness-for-Purpose Acceptance Criteria

The significance of defects can in general be assessed by fracture mechanics or large scale / wide plate tests, and is dependent on defect parameters like type, size and location, and on non-defect related parameters like stress, environmental factors and material properties. The severity of pipeline girth weld defects is determined from a number of factors and will be different for different application areas: Internal pressure and variations, laying forces, reeling forces, free spans and vibration, accidental loads, corrosion and erosion initiation, etc. For pipelines, absolute criteria are often based on critical defect sizes for plastic collapse, which are defect length, height, and wall thickness dependent.

Formulating NDE acceptance criteria for a fitness-for-purpose assessment is a much more difficult task than for quality control. In principle every individual defect, or combination of defects, which might lead to an unacceptable condition of a construction, or a high probability for this, should be revealed. In order to formulate acceptance criteria it will be necessary to take into account defect severity, for instance in the form of probability of failure as function of defect severity parameters, anticipated defect distributions, or distribution forms, - and the anticipated number of defects. A formulation might be based on the reliability updating achieved through NDE results. In order to compensate for the unreliability inherent in many NDE methods, this might, for a number of applications, lead to acceptance criteria close to those for traditional quality control.

Ideally, a fitness-for-purpose approach should not be made by evaluating a single NDE indication. NDE should first be performed, the defect contents then assessed based on the

NDE results, and acceptance or rejection of a construction as a whole (or defined part thereof) made from the combined severity of all defects present. Corrective actions as required should then be implemented. There is, however cases, for which this approach is not practical. One such important case is during offshore pipe lying, where time is short between welding and lowering of the pipe into the sea. A decision on acceptance or not of each weld has to be made within a short time window. An assessment of a pipeline as a whole is precluded. To meet this situation a special formulation of (discrete) defect or single weld based acceptance criteria has to be made reflecting the overall integrity of a pipeline.

3. Qualitative description of POD for MLF

3.1 Probability Calculations

The probability that a flaw is between x and $x + dx$ is $p(x)dx$

x is the flaw size

$p(x)$ is the probability density

$$\int_0^\infty p(x)dx = 1$$

$$x_a = \int_0^\infty x\,p(x)dx$$

x_a average flaw size

The probability that a flaw is smaller than x is $P(x)$

$$P(x) = \int_0^x p(x)dx$$

$P(x)$ cumulative probability

$$\lim_{x\to\infty} P(x) = 1$$

$$P(x_m) = 0.5$$

x_m median flaw size

3.2 Probability Calculations (POD)

The probability that a flaw of given size x is detected:

$$POD(x)$$

$$\frac{\partial POD}{\partial x} \geq 0$$

$$\lim_{x \to \infty} POD(x) = 1$$

The probability of detecting a flaw of size between x and $x + dx$ is

$$POD(x)\, p(x)\, dx$$

The probability of having an undetected flaw of size between x and $x + dx$ is

$$[1 - POD(x)]\, p(x)\, dx$$

After NDT, the modified probability density of the reduced ensemble

$$p'(x) = k[1 - POD(x)]\, p(x)$$

Re-normalization

$$\int_0^\infty p'(x)\, dx = 1$$

3.3 Probability Distributions

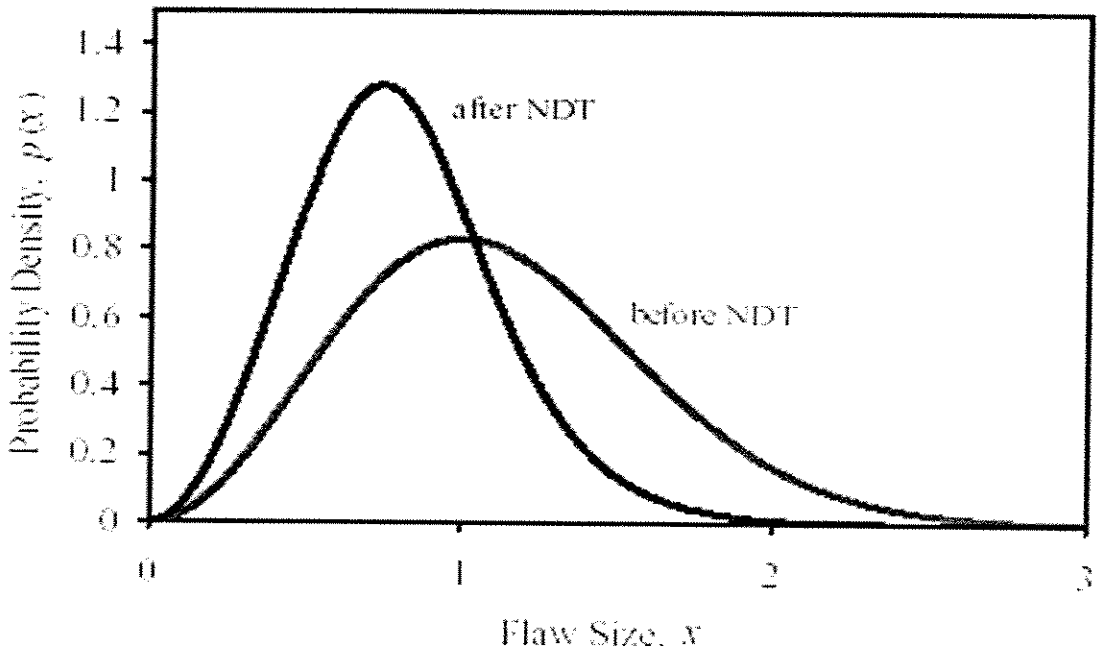

Fig 3.3.1: Probability density distribution of flaw size before and after NDT

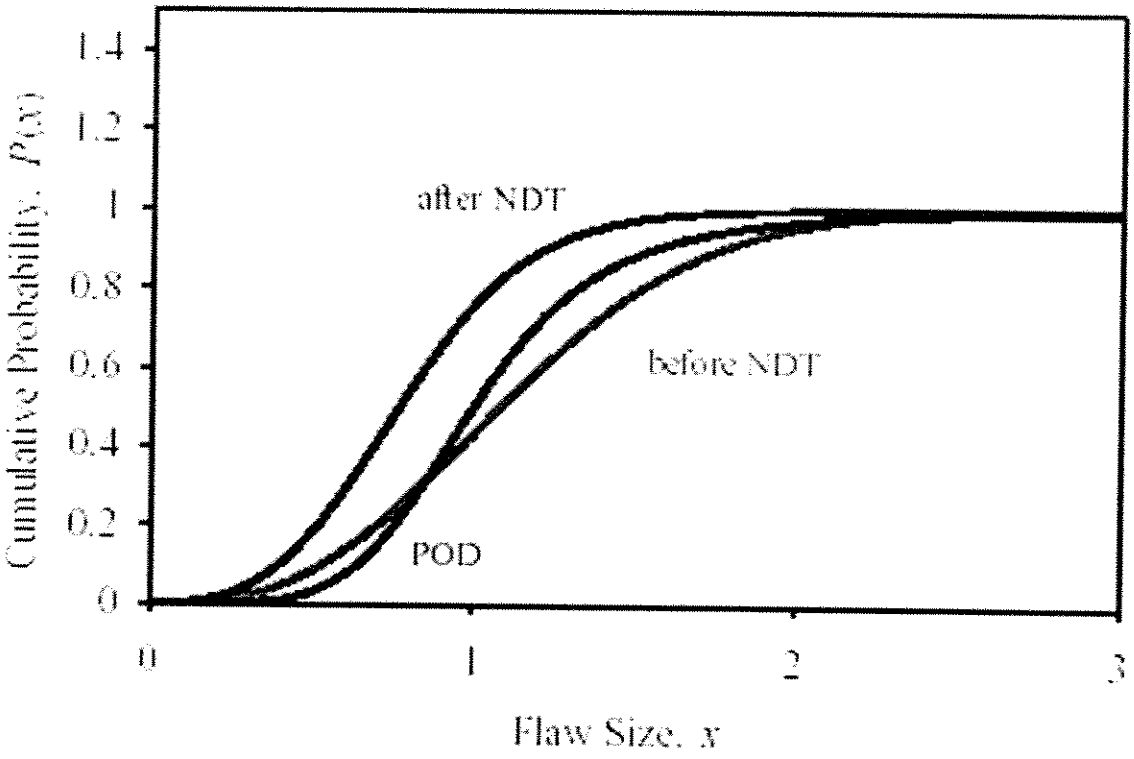

Fig 3.3.2: Cumulative probability density of flaw size before and after NDT (POD is shown)

3.4 Noise-Limited POD

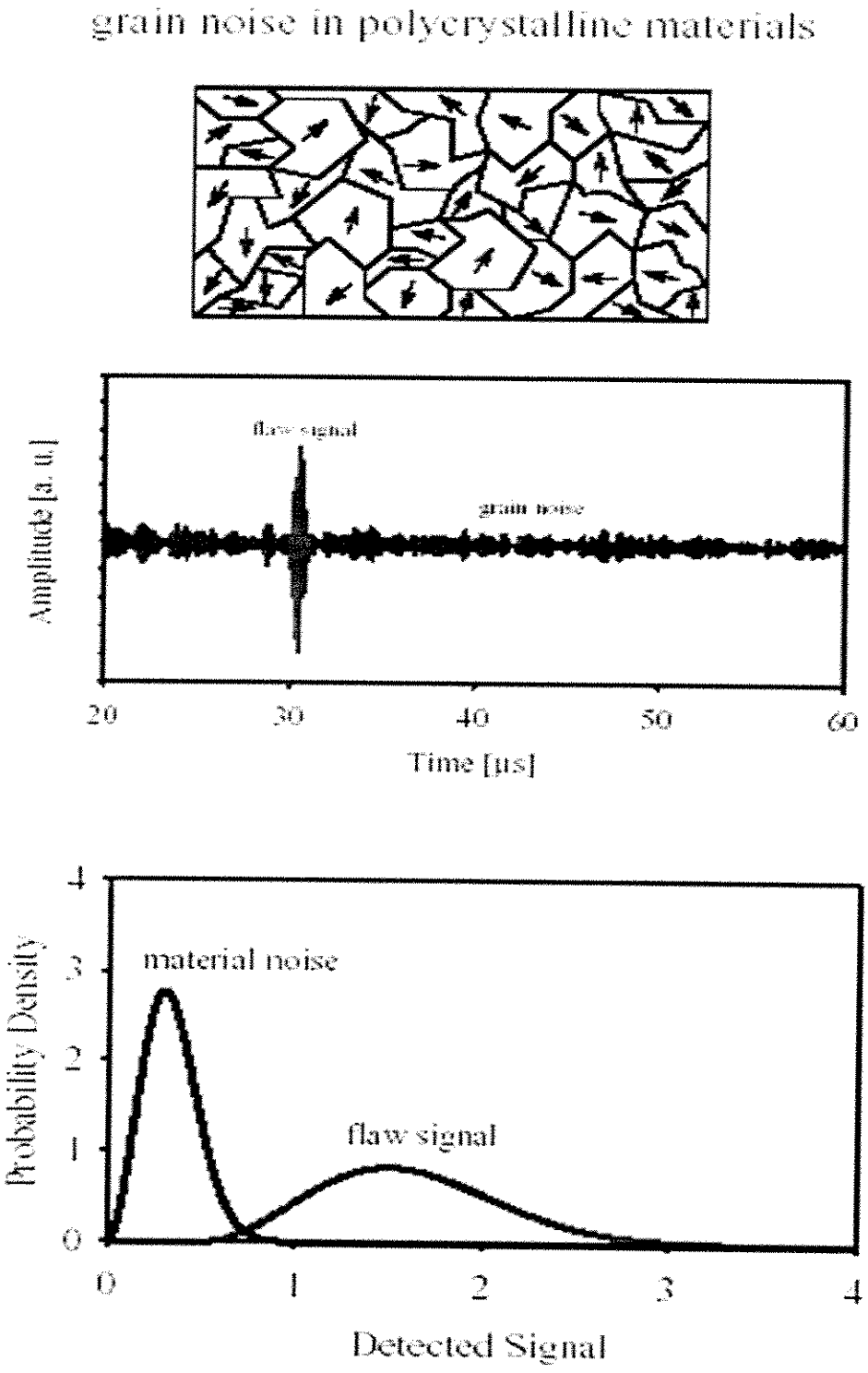

Fig 3.4.1, 3.4.2, 3.4.3: Effect of noise on signal detection

3.5 False Alarms versus Missed Flaws

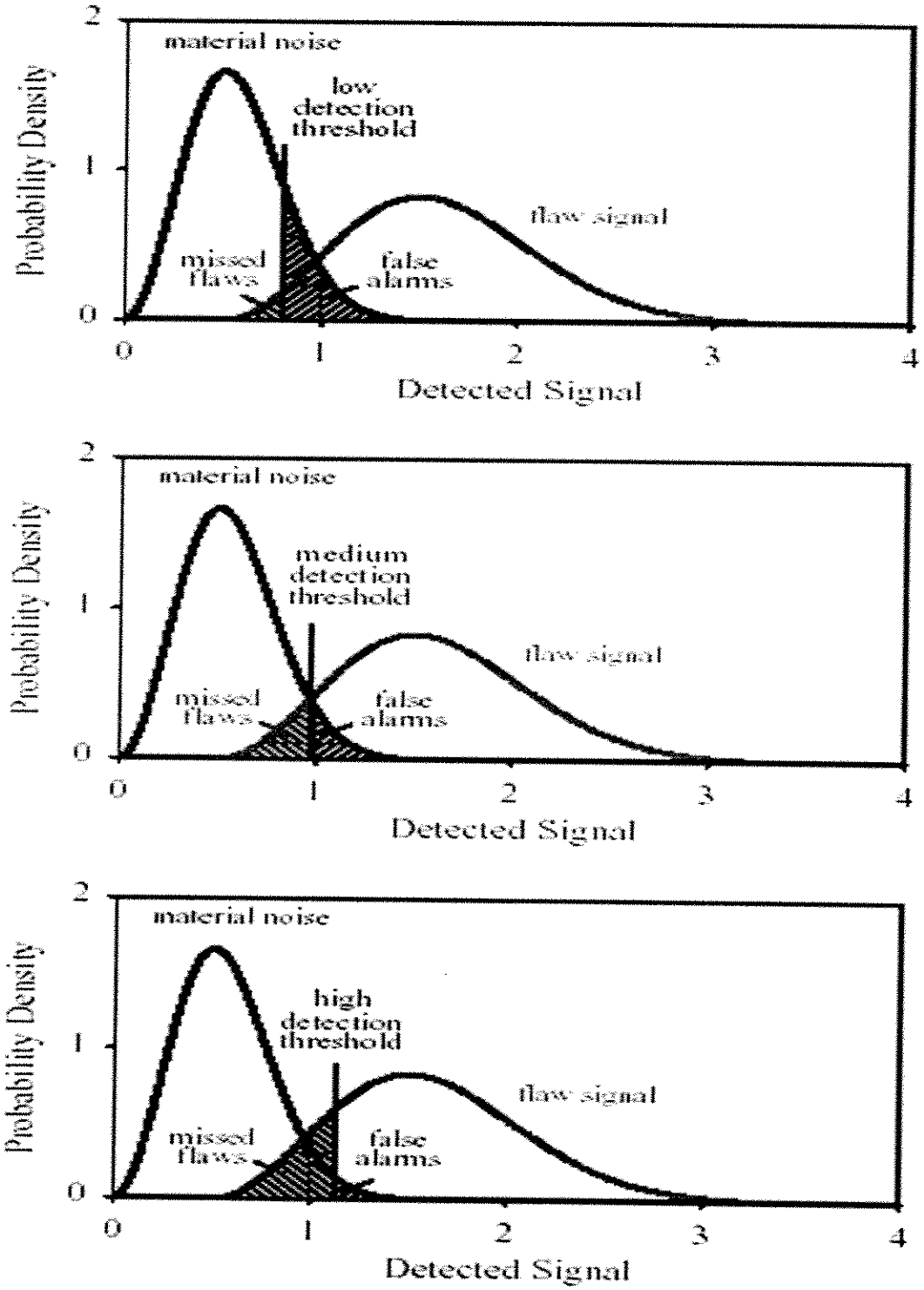

Fig 3.5: Different scenarios for varying POD and false alarms as function of high detectction threshold

III) Derivation of in-line instrumentation uncertainties.

Note: While in this section we were aiming at introducing accurate assessments and values for uncertainties from a specific vendor (Rosen) and to interpret them, the vendor could not supply us at the moment with the required data. The presented information come from published literatures.

1. Location Accuracy

Most MFL vendors report that their tools provide location accuracies to within 3 to 7 feet or within 0.1 to 0.3 percent of the distance from the nearest reference point. Inspection tools determine the location of an indication by odometer measurements from known reference points. So, the location accuracy of a tool depends on both the accuracy of the odometer and the location of the reference points.

One pipeline operator recently reported using magnetic reference markers points every 1.5 miles along a pipeline route. A 1.5-mile spacing and a 0.1 percent inaccuracy give an expected location accuracy of within 4 feet midway between the markers. There are few reports of location accuracy for actual MFL tools. An advanced tool vendor reported that 97 percent of indications were located within 5 feet of the actual condition.

Accurate pipeline drawings with detailed locations of valves, branch connections, and other pipeline features help improve location accuracy. By setting reference points (for example, magnetic markers) each mile or less, an inspection vendor can tailor the location accuracy of its tool to a required value. On lines with many clearly defined reference points, these accuracies can approach several inches.

No significant theoretical restrictions exist on location accuracy other than odometer inaccuracy. Odometer inaccuracies result wear and slip of the wheels.

2. Detection Thresholds

In general, the amplitude of a flux leakage field is related to the volume of metal loss. Therefore, the threshold of detection or minimum detectable metal-loss region for MFL tools is related to the length, width, and depth of the region.

Several reports have been published giving thresholds of detection for MFL tools. For conventional tools, vendors state that the smallest detectable corrosion pits have depths between 15 and 20 percent of the wall thickness. Similarly, the smallest detectable pits have lengths and widths that are 80 percent of the wall thickness. For advanced tools, the smallest detectable corrosion pits are reported to be 20 to 40 percent deep for one vendor and 20 to 70 percent deep for another. The 20 percent depth refers to corrosion patches with a length and width equal to three times the pipe wall thickness; the 40 to 70 percent depths refer to pits that are one-third smaller.

Theoretically, the detection threshold should be a function of the flux leakage amplitude compared to the noise and background signal level. Typical pipeline steels have background noise levels of about 3 gauss, but the noise can be as high as 15 to 20 gauss.

Detection thresholds depend on the signal-to-noise ratio. A small 10 percent deep defect produces a signal that is larger than typical noise levels, but a small 5 percent defect produces a signal that is lost in the noise. So, detection thresholds of 10 percent are attainable for most pipeline steels. Lower thresholds are only possible in quiet steels, and larger thresholds are likely in noisier steels.

3. Probability of Detection

Most conventional tool vendors do not publicly show information on expected probabilities of detection levels. These data are considered proprietary. When published, a single probability of detection value or confidence level is generally given, rather than both.

One advanced tool vendor reports a confidence level of 80 percent for metal-loss anomalies with a length or width greater than the wall thickness of the pipe. This confidence level includes false calls as well as missed defects. So, the actual confidence level on detection may be higher. Several advanced tool vendors report confidence levels that depend on the size of the metal-loss region; one vendor gives a 40 percent confidence level for a region with a length or width equal to the wall thickness and 95 to 99 percent for a region that is three times larger.

In one published report for an advanced tool, a pipeline operator reported on the results of a trial where a tool was run through a line with 79 metal-loss defects. These metal-loss regions consisted of corrosion pits ranging in depth from 14 to 61 percent deep and corrosion patches from 11 to 52 percent deep. All metal-loss regions were detected, and no false calls were reported. An advanced tool vendor also reported on a program where 33 indications were investigated. All of the indications reported by the tool existed, and there were no false indications.

Theoretically, the probability of detection should be set by the magnitude and spread of leakage signals compared to the background signals. If the leakage field is well above the noise and background level, the probability of detection should be near 100 percent. At or near the noise and background level, the probability of detection should drop significantly.

An important consideration in determining the probability of detection during an actual inspection is the presence of "blind spots" or areas where the pipe is not inspected. Blind spots can occur due to excessive speed, sensors bumping off the pipe wall, deposits inside the pipe, sensor failures, electronic failures, and the capabilities of the inspection log analyst or analysis program. Depending on the capabilities of a tool, the presence of blind spots can strongly impact the true probability of detection.

4 Characterization of Metal-loss Defects

Once a defect is detected, its signal must be analyzed to determine the defect's potential effect on the operation pipeline. Because there is not a simple and direct transformation between flux leakage and defect geometry, many methods have been developed to interpret MFL signals and characterize the geometry of defects. These methods include template matching, statistical methods, and neural networks. Each method has had varying degrees of success, and each has its own strengths and weaknesses.

The development of a characterization method using statistical methods illustrates the many of issues associated with characterization functions. The most commonly used method of analyzing MFL signals is to make inferences or calculations based on features of the signals.

To determine realistic estimates of the capability of such methods, classical mathematical modeling techniques were used to develop characterization algorithms. First, features of signal, such as peak amplitude, signal duration and sensors responding, were extracted from the recorded flux leakage response. Then statistical methods were used to establish characterization and compensation algorithms.

5. Depth Accuracy

Some inspection tool vendors report defects by categories or ranges of depth or severity. Severe or "Class 3" defects often have an estimated depth greater than 50 percent of the wall thickness. Moderate or "Class 2" defects have depths between 25 and 50 percent or 30 to 50 percent. Light or "Class 1" defects have depths up to 25 percent or from 15 to 30 percent. When accuracies on the classes are reported, they are typically reported to be within 10 percent of the wall thickness.

Other tool vendors report an estimated depth, rather than a broad classification of severity. The reported accuracies are typically ±10 percent of the wall thickness with a confidence level of 80 percent. For some advanced tools, software is used to invert the measured signals, providing a contour map of the signal amplitude. These contour maps may be calibrated to be proportional to the defect depth. The inversion process often uses the same basic amplitude-depth relationships used for conventional-tool analyses.

The statistical analyses performed for the gas institute suggests that depth accuracy of 8 percent of the wall thickness (with 95 percent confidence) is ultimately possible for elliptical defects less than 50% deep. However, an accuracy this high could not be obtained. Accurate depth estimation is possible only when the analyses are appropriately compensated for other geometry variables. The best accuracy obtained in the analyses is ±19 percent (for a 50 percent deep defect and with 95 percent confidence). Most of the error is likely due to the width estimation procedure used in the analyses, although it is not clear that better methods exist.

The statistical analyses suggest that defect parameters, such as the width-to-length ratio, are particularly important when estimating depth. If depth predictions are made on amplitude alone - that is, if these other parameters are not taken into account - the accuracy plummets. The magnitude of depth estimation error increases with increasing defect depth. Depth estimation can be improved by compensation for inspection variables, but the impact of inspection variable compensation is small compared to geometry compensation for the range of variables considered in this study.

Confidence levels are particularly important in defining accuracies. At lower confidence levels (e.g., 80 percent, a commonly reported confidence level), the accuracy appears much greater. A 95-percent confidence level implies that 19 out 20 defects (95 percent) are reported within the tolerance given. An 80-percent confidence level implies that 16 out of 20 defects are correctly reported.

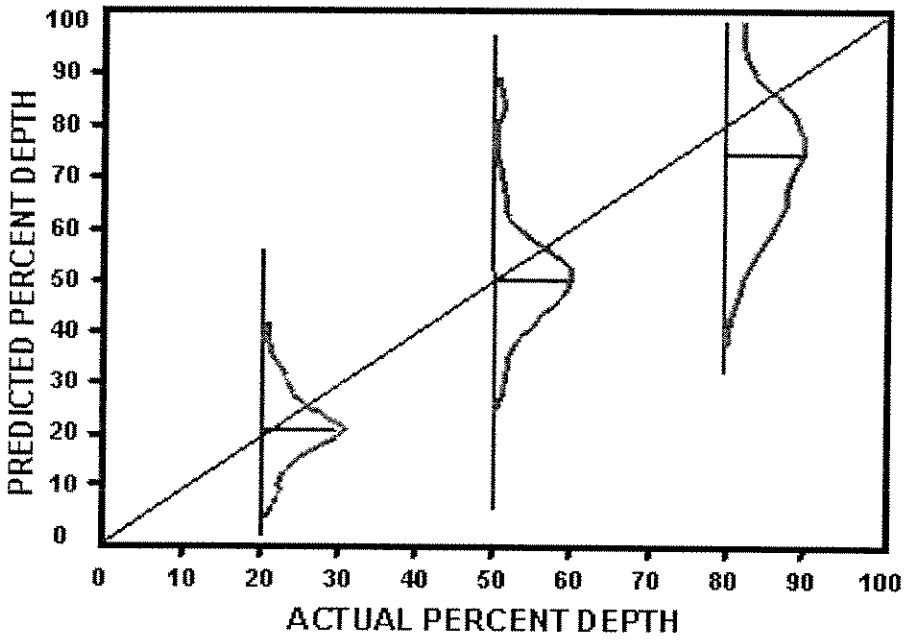

Fig 1: distribution of predicted depth vs actual depth for different depths

Compensation for Background Magnetization & Velocity?	No Compensation for W/L	Compensated for True W/L	Compensated for Estimated W/L
No Compensation for Background Magnetization or Velocity	First Generation	Optimal	Second Generation
Compensation for Background Magnetization and Velocity	Advanced First Generation	Optimal	Advanced Second Generation

Table 1: depth estimating procedures

Compensation for Background Magnetization & Velocity ?	True Depth (%)	95% Prediction Interval for Estimated Depth (%)		
		No Comp. for W/L	Comp. for True W/L	Comp. for Estimated W/L
No Compensation for Background Magnetization or Velocity	20	15 +/- 15	22 +/- 9	21 +/- 12
	50	52 +/- 50	49 +/- 10	50 +/- 20
	80	69 +/- 47	76 +/- 16	74 +/- 23
Compensation for Background Magnetization and Velocity	20	16 +/- 14	22 +/- 7	22 +/- 11
	50	52 +/- 49	49 +/- 8	50 +/- 19
	80	71 +/- 44	79 +/- 12	77 +/- 21

Table 2: Results for different combination of compensations

6. Width Accuracy

Width is not commonly reported by inspection vendors, and when it is, it is typically based on the width of the recorded MFL signal. Most, or all, inspection vendors do not report accuracy of their width estimates. Because width-to-length ratio significantly affects the ability to predict depth, accurate width estimates are important.

The statistical analysis performed in this project suggests that width accuracy of ±1.5 to 2 inches (with 95 percent confidence) is possible for defects with widths from 1 to 6 inches. Accuracies as low as ±2 to 4 inches are likely with unsophisticated analysis procedures. As with depth estimation, errors in width estimation are due primarily to defect geometry (and/or permanent local pipe conditions).

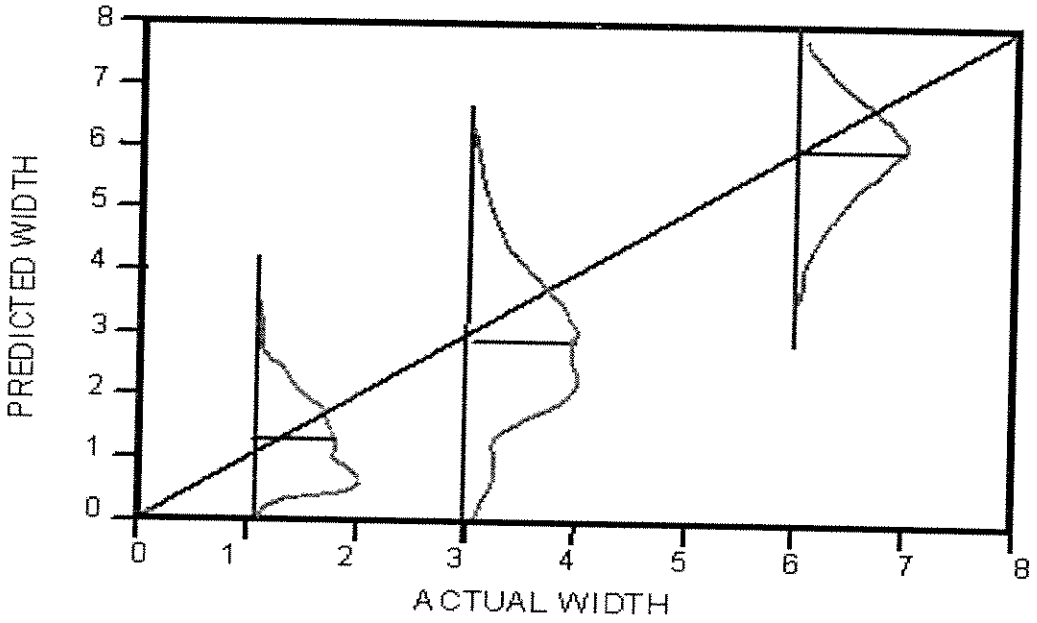

Fig 2: distribution of predicted width vs actual width for different widths

7. Length Accuracy

The length of individual defects is commonly reported by inspection vendors. Reported accuracies are typically with 0.25 to 0.5 inch with no claim on confidence level.

The statistical analysis performed in this project suggests that individual defect length can be estimated quite well without compensation for other features. In fact, an individual defect's length seems to be the geometry characteristic most accurately estimated, at least for individual defects. Methods were developed that provided length estimation errors of approximately +/- 1 inch (25.4 mm) with 95% confidence. Improvements come at the cost of defect detection capability.

The errors in length estimation are due primarily to defect geometry (and/or permanent local pipe conditions) and random error, with the two factors switching relative importance with increasing length. Almost no unexplained length variability is attributable to inspection conditions. The defect geometry effects are especially important when multiple defects are in close proximity to each other. While not explicitly evaluated in this study, the accuracy with which the length of individual defects in close proximity to others is expected to be low.

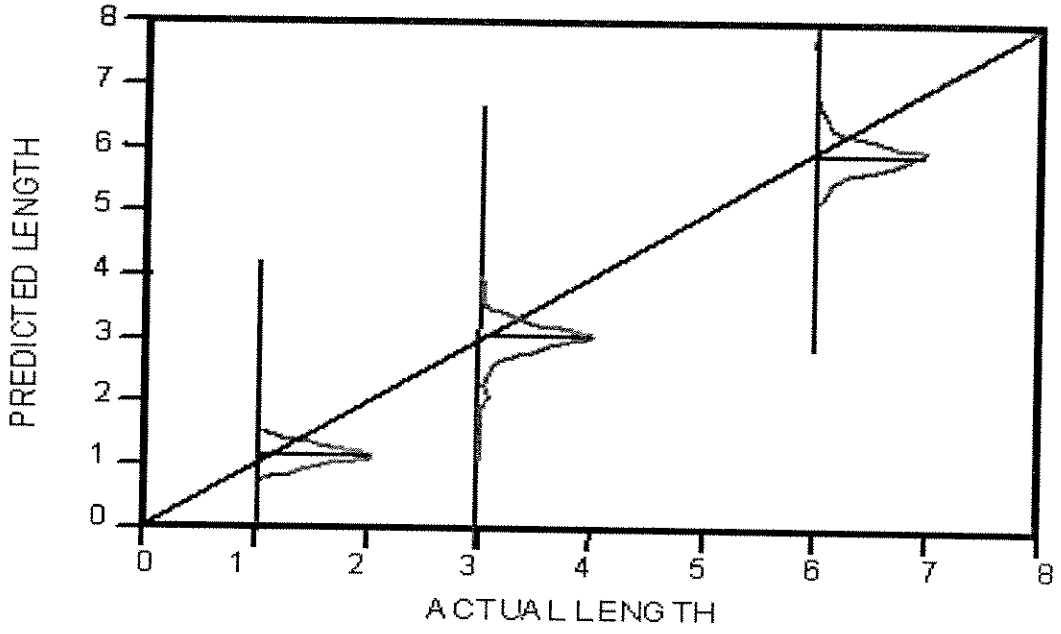

Fig 3: distribution of predicted length vs actual length for different lengths

8. Comments

8.1 Current Detection Capabilities

MFL can detect metal-loss defects in pipelines with good confidence, but operational considerations restrict its use in some pipelines. These restrictions are not limitations of MFL per se. Rather they result from physical constraints such as reduced port valves, or normal variations in operating conditions such as product flow speed. Most metal-loss regions produce a measurable flux leakage that is detectable with typical MFL tools, even for small imperfections that do not threaten the structural integrity of a pipeline.

For very shallow, long, or narrow metal-loss regions, the MFL signal can become hard to detect. Extremely narrow defects (for example, electric resistance seam weld corrosion or stress-corrosion cracks) do not produce measurable signals in typical MFL systems. Also,

background noise levels and variations in tool speed and remaining magnetization impact the detection threshold. These operational variations occur, for example, after the MFL tool exits a bend or restriction, at which time the tool speed can be quite high.

8.1 Current Detection Capabilities

Metal-loss defects can generally be detected with MFL tools, but characterization accuracy is also important. Analyses to determine the maximum safe operating pressure of a pipeline require information on the depth, length, and shape of metal-loss regions. As a result, characterization accuracy plays a strong role in an MFL tool's ability to provide results that can be used to estimate maximum safe operating pressures.

The ability of an MFL tool to characterize the depth, shape, and length of a metal-loss region depends on the size of the sensors and the sophistication of the data analysis system. Conventional MFL tools have a limited potential for characterizing defects because they typically use large sensors and manual (noncomputerized) analysis systems. Advanced or high-resolution MFL tools, with small sensors and computerized analysis systems, have the potential for more accurate characterization.

The characterization accuracy of most MFL tools is highly variable. Most vendors report sufficiently high accuracy on depth and length predictions of individual defects to make accurate serviceability calculations. However the confidence level of the measurement can mean a significant number of defects will not be properly characterized. For example, many vendors state a depth accuracy of ± 10 percent of wall thickness and a length accuracy of ± 0.5 inches (12mm) with a confidence of 80 percent. That is one out of every 5 defects will be characterized incorrectly. This lack of confidence is due to the inherent problems associated with the prediction of defect geometry.

Complex shapes, long and narrow grooves, multiple pits, and inspection variables present analysis problems for either the inspector or computer analyzing the log. As a result, it is difficult for pipeline operators to estimate the maximum safe operating pressure of a pipeline on the basis of current MFL inspection reports. For groups of defects or defects within other defects, it is not likely that an accurate ranking of defect severity can be made using present technology. Improved characterization accuracy of MFL tools would allow pipeline operators to better understand the likely severity of reported anomalies. However, there will be an ultimate limit to characterization accuracy.

High characterization accuracy is not always needed. The required accuracy depends on the goal of the inspection and on the number of indications found. On lines with few indications, high characterization accuracy may not be needed if all indications are independently investigated. Conversely, where access to the line is difficult and on lines with many indications, characterization accuracy may be far more important, especially in critical areas. In addition, the required characterization accuracy depends on the depths of the metal-loss regions found. Inaccuracies in estimating the remaining wall thickness directly impact the estimated severity of a metal-loss anomaly. For deep metal-loss regions, errors in depth strongly affect calculated severity for defects. For shallow regions, errors in depth are less important.

IV) Probability of failure calculations

This section is mainly covered by the development of the excel program. I will present some information on how the program works (logical algorithm). Please refer to the appendix a for the user guidelines and to chapter VI) of the report for an example.

The user will enter information about width and length. The user has to input real values of width and length given a certain pig measurement. For ex: given a width measurement of 2t (2*thickness) from the pig, the median real width is 1.9t for example with a 10% coefficient of variation, and given a width measurement of 2.5t (increments of 0.5t for width and length), the real median width is 2.6t with 15% coefficient of variation. (the median real width and coefficient of variations are obtained from statistics done by pig vendors on their tools. The same thing is asked for Length of the defect. This will allow the program to correct for uncertainties related with pig measurements. So if the user will later enter a measured defect width value of 2.2t, the program will corrected by interpolating it between the "real" interval of 1.9t (associated with a measurement of 2t), and 2.6t (associated with a measurement of 2.5t). Also interpolation is done for the coefficient of variation.

Based on values of width and length, a defect is than classified to be a pitting defect, general pitting, circumferential grooving and axial grooving. For each of these categories, the user is asked to enter information about the POD (cumulative probability of a detected defect does exists given a pig call), the median defect depth and its coefficient of variations for different intervals of defect depth d (same principle of width calibration explained above). Thus the program will identify a defect (pitting...) and than interpolate to get the median actual value of the defect depth as well as the coefficient of variation and the POD.

Having corrected all measurement errors for width, depth and depth, and given that the user is asked to input pipe information (diameter, thickness, SMYS...), the program will use the corrected measurements to calculate the burst pressure for the three models (RAM, B31G, and DNV). Please refer to Chapter II (literature review), section 3 for more information about these models. It should be noted that for the B31G model, the program uses the factor of safety of 0.72 as specified by the model. Some analyst however might choose to ignore the factor of safety for analysis purposes (not design).

After calculating the burst pressures, and since the user is asked to input demand information as well as biases on both demand and capacities, the program calculates the probability of failure of the detected defects assuming a lognormal distribution for all parameters. The probability of failure for the detected defects will be equal to:

Pf = POD*Pf of detected defect +(1-POD) Pf (statistics).

Pf statistics comes from the following:

In fact in order to assess the probability of failure of sections where no detection occurs. The program offers to approaches:

First, it does a statistics on the detected defects and uses the median values of width, length and depth and their respective coefficients of variations for burst pressure calculations. Than the probability of failure is calculated based on lognormal assumptions for the parameters.(pf statistics)

Second, the user is also asked to enter median expected depth, width and length from corrosion models. The program than calculate the Pf based on these values and that is called (Pf prediction)

The user is advised to use the most conservative value from Pf statistics and Pf prediction.

V) Testing corrected models with a real example

A) Inputting data

The developed program was tested using data form line 25 inspection. (Appendix c)
The program assumes lognormal distribution for all parameters.
The following information's about demand, capacity. Pipeline characteristics and material strength were provided for the line 25: (tables 1,2 &3)

Pipeline Characteristics (median values)				Steel Material Strengths (median values)			
Diameter, D_{50}	$V_{D,I}$	Wall Thickness, t_{50}	$V_{t,I}$	Yield Strength, YS50	$V_{YS,I}$	Tensile Strength, TS_{50}	$V_{TS,I}$
Inches		Inches		PSI		PSI	
8.625	10%	0.5	12%	42000	8%	52000	8%

Demand information			
Median demand (psi)	Type I uncertainty	Median Bias	Type II uncertainty
5186	10%	1	0%

Capacity biases					
RAM		B31G		DNV	
Median Bias	V%	Median Bias	V%	Median Bias	V%
1	34%	1.52	36%	1.48	57%

Tables 1,2 &3: Pipeline information.

While detailed use of the spreadsheets is explained in the users guidelines (appendix a), we will go step by step inputting data is this example in order to illustrate the proper use of this program.
All colored cells represent cells were data need to be inputted. All these cells are present in "sheet 1" of the excel program, which is the user spreadsheets. The rest are for calculations.
Since no valuable information regarding pig measurement uncertainties was provided, we assumed for this example that the pig is accurate (measured defects = real defects and no variations). This also implies that there is no distinction between the different types of defects (pitting, grooving) in term of detection accuracy, or POD (cumulative probability of detection/ pig call), and anyway such information was not provided. So POD was assumed to be 1, meaning that given a call, the call is right and the defect exists. (Tables 4 &5), and measured defect depth, width and length are equal to real depth, width and length.. (tables 4, 5, & 6)
Table 6 also shows where to input field data from pig inspection (pig location, defect size in term of depth, width and length as a percentage of nominal wall thickness).

Measured	Real data for General pitting				Real data for Pitting defect			
d (X*t)	POD	Median d	Vd(fraction)	Vtc(fraction)	POD	Median d	Vd(fraction)	Vtc(fraction)
0	1	0	0	0	1	0	0	0
0.1	1	0.1	0	0	1	0.1	0	0
0.2	1	0.2	0	0	1	0.2	0	0
0.3	1	0.3	0	0	1	0.3	0	0
0.4	1	0.4	0	0	1	0.4	0	0
0.5	1	0.5	0	0	1	0.5	0	0
0.6	1	0.6	0	0	1	0.6	0	0
0.7	1	0.7	0	0	1	0.7	0	0
0.8	1	0.8	0	0	1	0.8	0	0
0.9	1	0.9	0	0	1	0.9	0	0
1	1	1	0	0	1	1	0	0

Real data for Axial Grooving				Real data for Circumferential grooving			
POD	median d	Vd(fraction)	Vtc(fraction)	POD	median d	Vd(fraction)	Vtc(fraction)
1	0	0	0	1	0	0	0
1	0.1	0	0	1	0.1	0	0
1	0.2	0	0	1	0.2	0	0
1	0.3	0	0	1	0.3	0	0
1	0.4	0	0	1	0.4	0	0
1	0.5	0	0	1	0.5	0	0
1	0.6	0	0	1	0.6	0	0
1	0.7	0	0	1	0.7	0	0
1	0.8	0	0	1	0.8	0	0
1	0.9	0	0	1	0.9	0	0
1	1	0	0	1	1	0	0

Tables 4 and 5: POD and measurements uncertainties information's.

						Pig data			
						Feature characteristics			
W (X*t)	median W	V(W)	L (X*t)	median L	V(L)	Distance (ft)	Depth(X*t)	width(X*t)	Length (X*t)
0	0	0	0	0	0	39.505	0.250	2.126	3.308
0.5	0.5	0	0.5	0.5	0	39.739	0.120	2.048	3.308
1	1	0	1	1	0	39.781	0.100	1.732	2.678
1.5	1.5	0	1.5	1.5	0	40.124	0.150	2.284	4.330
2	2	0	2	2	0	40.138	0.230	2.44	3.150
2.5	2.5	0	2.5	2.5	0	40.195	0.190	2.914	3.780
3	3	0	3	3	0	40.199	0.120	2.284	2.756
3.5	3.5	0	3.5	3.5	0	40.439	0.120	1.968	2.834
4	4	0	4	4	0	40.454	0.370	2.204	3.386
4.5	4.5	0	4.5	4.5	0	40.696	0.120	2.756	4.174
5	5	0	5	5	0	40.717	0.100	1.812	1.732
5.5	5.5	0	5.5	5.5	0	41.945	0.200	1.968	3.150
6	6	0	6	6	0	42.185	0.100	1.968	2.440
6.5	6.5	0	6.5	6.5	0	42.371	0.140	1.89	2.520
7	7	0	7	7	0	43.692	0.340	2.204	7.560
7.5	7.5	0	7.5	7.5	0	44.441	0.230	2.678	3.228
8	8	0	8	8	0	92.421	0.130	2.678	1.102
8.5	8.5	0	8.5	8.5	0	111.863	0.450	1.496	4.724
9	9	0	9	9	0	275.545	0.490	2.362	11.968
9.5	9.5	0	9.5	9.5	0	856.807	0.420	2.834	3.544
10	10	0	10	10	0	1361.224	0.470	2.284	4.410
10.5	10.5	0	10.5	10.5	0	1486.085	0.100	2.126	2.598
11	11	0	11	11	0	1569.664	0.140	0.866	5.040
11.5	11.5	0	11.5	11.5	0	1611.383	0.460	2.756	3.150
12	12	0	12	12	0	1653.234	0.100	2.204	2.520
12.5	12.5	0	12.5	12.5	0	2194.626	0.420	2.52	3.150
13	13	0	13	13	0	2320.538	0.380	1.89	2.834
13.5	13.5	0	13.5	13.5	0	3427.530	0.280	1.26	2.440
14	14	0	14	14	0	4592.774	0.130	1.812	2.362
14.5	14.5	0	14.5	14.5	0	4717.281	0.370	2.44	3.308
15	15	0	15	15	0	5983.869	0.380	1.654	3.150
						6475.969	0.310	1.968	3.386
						6597.481	0.220	1.182	2.834
						8052.064	0.370	1.496	3.622
						8506.312	0.110	1.418	1.654
						8506.404	0.240	1.418	1.732
						8643.035	0.180	0.944	1.654
						8643.807	0.150	1.102	2.362
						8643.955	0.110	1.182	1.812
						8644.392	0.130	1.024	1.418
						8644.596	0.200	1.418	2.126
						8645.677	0.100	1.812	1.260
						8647.784	0.100	1.812	2.048

Table 6: Width and length corrections as well as pig data

Uncorroded Pipe data provided in tables 1,2 &3 are than inputted in corresponding cells in tables 7, 8 and 9. Those data are about median initial wall thickness (in) , material properties(ksi), initial diameter(in) and their respective coefficients of variations.
Pressure data are also to be inputted and the program allows the user to input the median pressure (ksi) and its coefficient of variation for any location along the pipeline (in the example, a median pressure of 5.186 ksi was inputted with 10% coefficient of variation for all locations).
Capacity and demand biases and their variations are to be inputted (tables 8 and 9) for the three prediction models: RAM, B31G and DNV

Pipe data								Pressure data	
t nominal(in)		SMYS (ksi)		SMTS(ksi)		diameter D(in)			
Median	V(fraction)	Median	V(fraction)	Median	V(fraction)	Median	V(fraction)	Median (ksi)	V(fraction)
0.5	0.12	42	0.08	52	0.08	8.625	0.1	5.186	0.1
								5.186	0.1
								5.186	0.1
								5.186	0.1
								5.186	0.1
								5.186	0.1

Table 7

Capacity bias					
RAM		B31G		DNV	
Median	V	Median	V	Median	V
1	0.34	1.52	0.36	1.48	0.57

Demand bias					
RAM		B31G		DNV	
Median	V	Median	V	Median	V
1	0	1	0	1	0

Tables 8 and 9: Demand and capacity biases

Finally, based on the age of the pipelines, and with the use of appropriate corrosion prediction model (the one used in this example is described in appendix d), enter the expected median corrosion depth and coefficient of variation (table 10). These values will be used to assess the probability of failure of the sections of the pipeline where no defects were detected. This program also allows assessing the probability of failure of the sections of the pipeline where no defects were detected by the use of a statistics on the detected defects and apply them where no defects are detected. Values from the statistics and the prediction are to be compared, and the most appropriate or conservative value is advised to be used.

Median d(in)	V
0.17	0.2

Median W(in)	V
0.5	0.2

Median L(in)	V
0.5	0.2

Table 10: Expected corrosion depth, width and length.

B) Test Results

Test results from the program for line 25 were consistence with results from the POP report. It should be noted however, that the values might be slightly "shifted down" due to the use of slightly different pipe information (SMYS...) and no biases were included in the burst pressure (Pb) calculations, but were included in the Pf calculations.
Fig shows the burst pressure predictions for the detected defects from the three models. They match with those from the POP report. B31G appear low because of the use of the safety factor of 0.72 in the program.

Fig 2 shows Ram prediction of Pb for the detected defects, and non-detected defects. The non-detected effects Pb comes either from statistics (Pb stat), or form prediction (Pb predictions). The prediction values for Pb from Ram appear to be more conservatives.

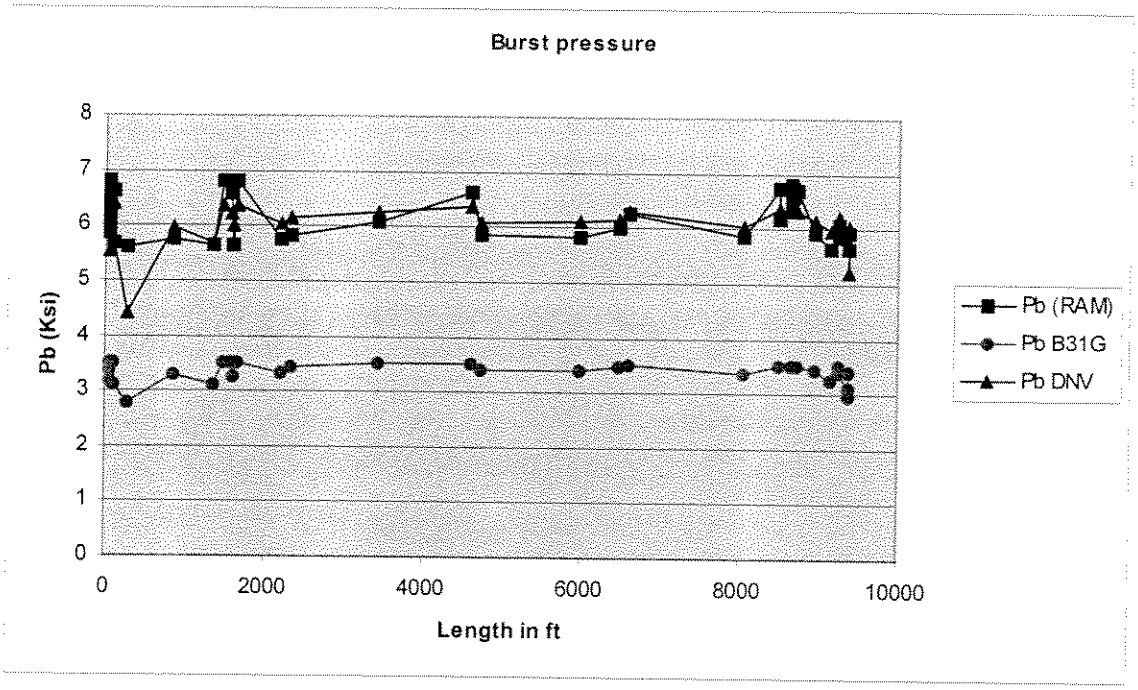

Fig 1: Detected defects burst pressures from the three models

Fig 3 and 4 show respectively B31G and DNV predictions for Pb of detected and non-detected defects. While it appears that B31G and DNV have relatively "high" Pb predictions from the non detected defects compare to RAM, this is mainly due to the fact that RAM Pb predictions decrease quickly for low values of the defect depth d, while B31G and DNV Pb predictions are almost insensitive for low defect depth. As we now, from the line 25 data, the median defect depth falls in the low range (around 0.1 inches) explaining this behavior (Fig 5 and 6)

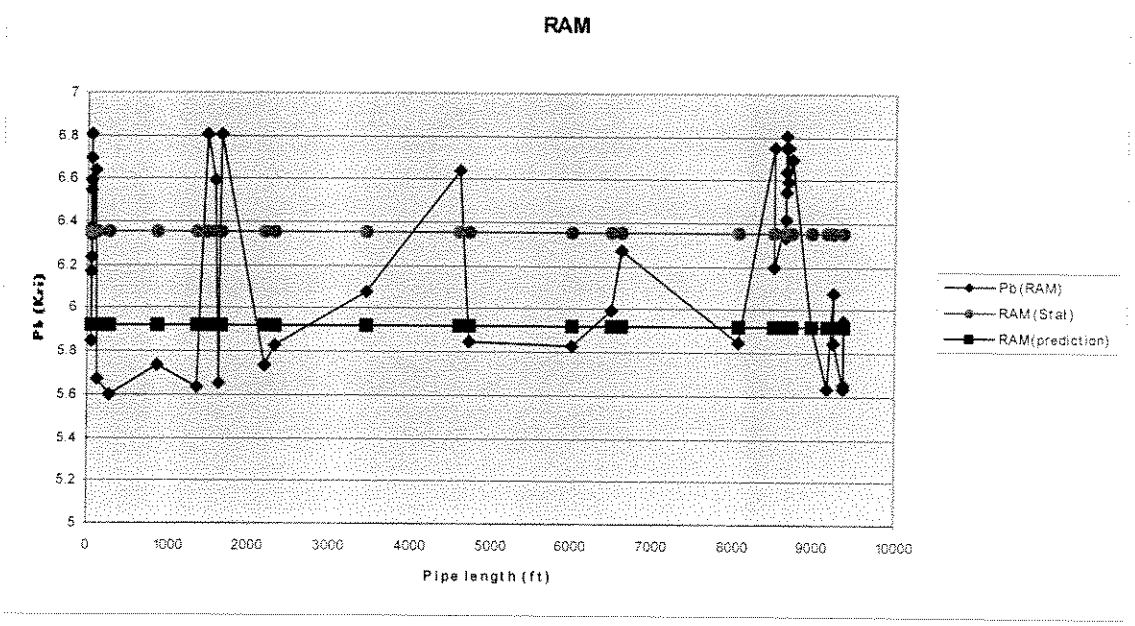

Fig 2: Ram estimates of Pb for the detected defects, and non-detected defects.

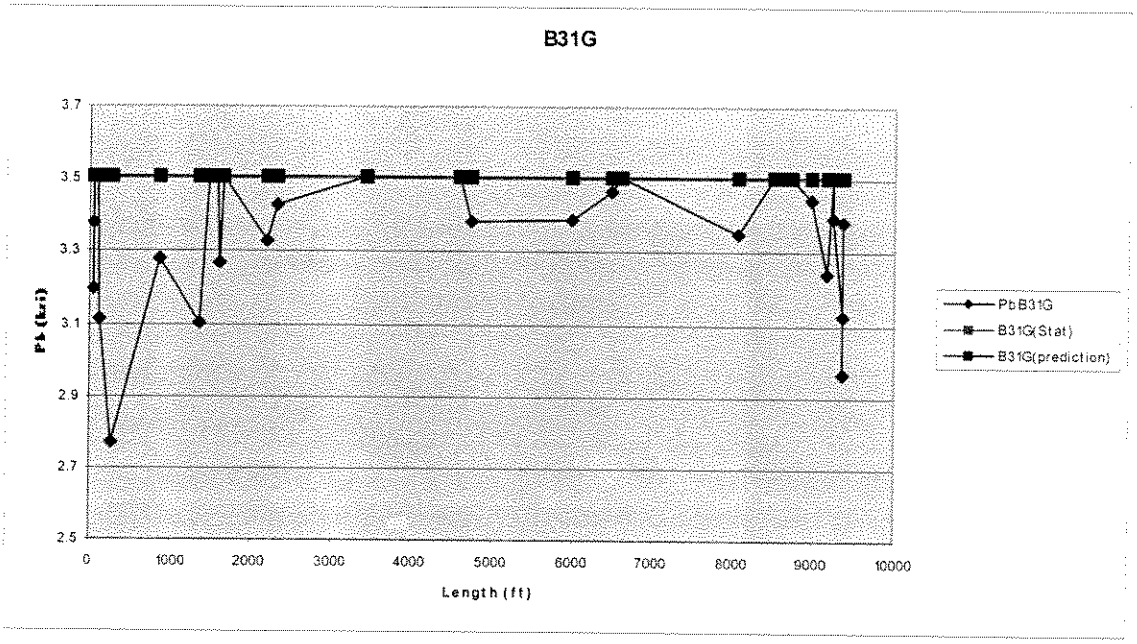

Fig 3: B31G estimates of Pb for the detected defects, and non-detected defects.

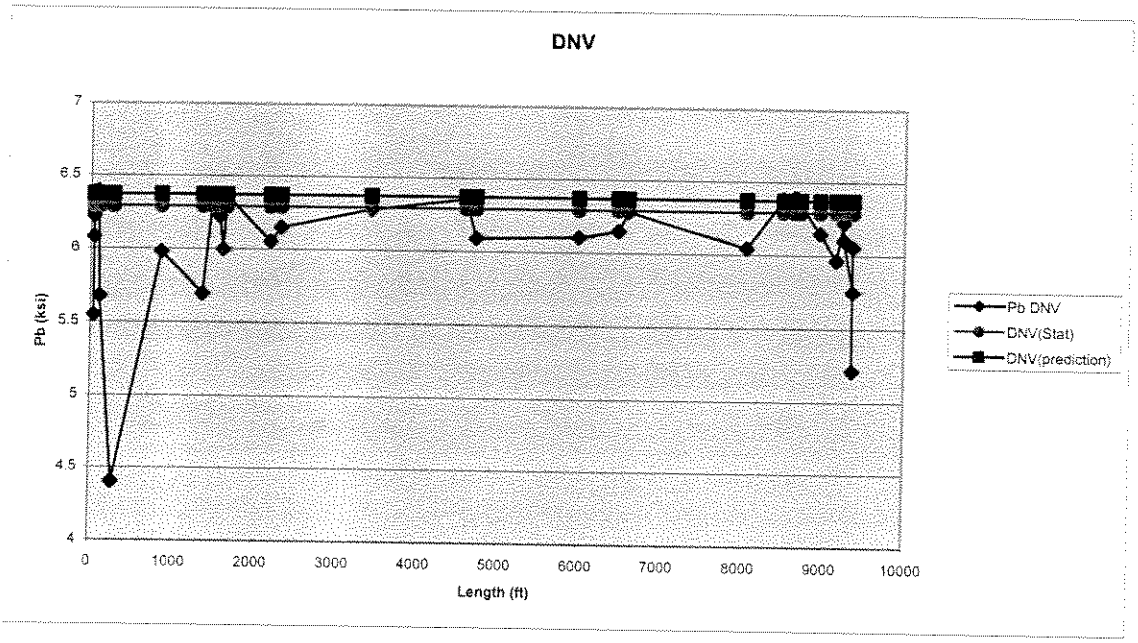

Fig 4: DNV estimates of Pb for the detected defects, and non-detected defects.

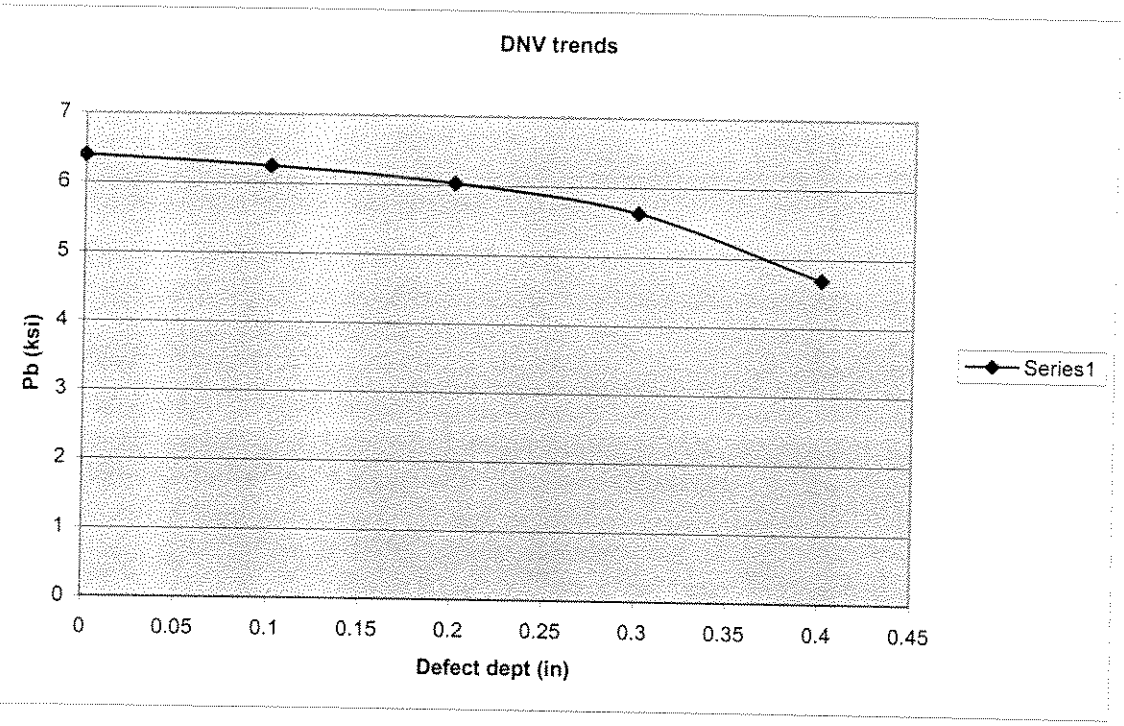

Fig 5: DNV trends of Pb change with different defect depth. (Other parameters fixed)

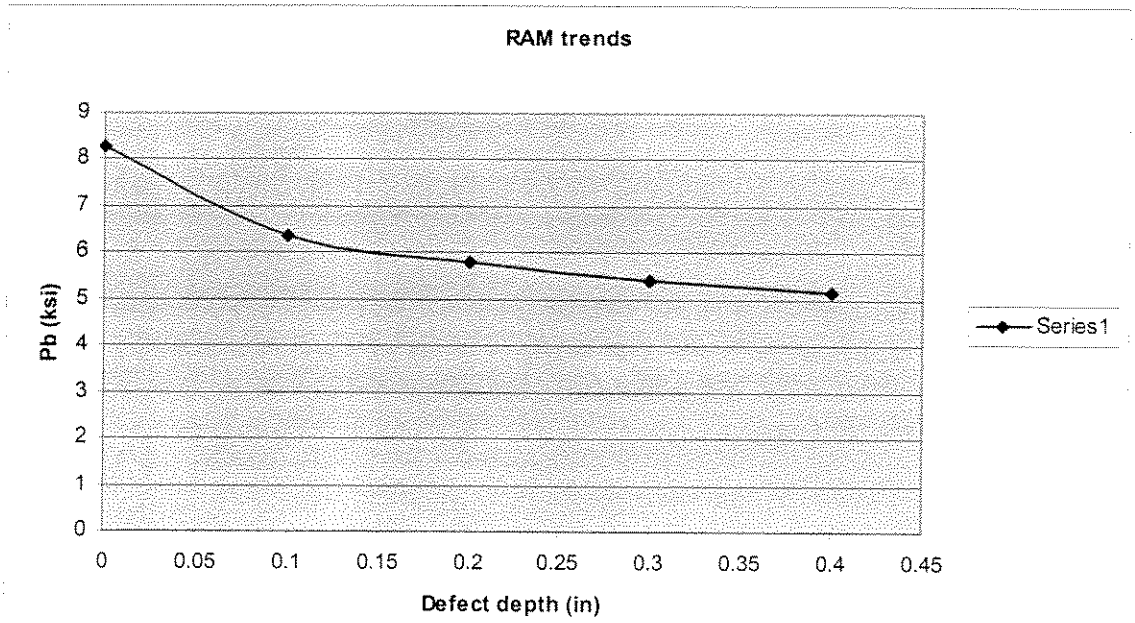

Fig 6: RAM trends of Pb change with different defect depth. (Other parameters fixed)

Pf calculations confirm the Pb calculations: the model estimating the lowest Pb (B31G) gave the highest probability of failure (fig 7). The large significant difference between the Pf from statistics and the pf from predictions for DNV although the Pb are almost equal is due to the differences in coefficients of variations.

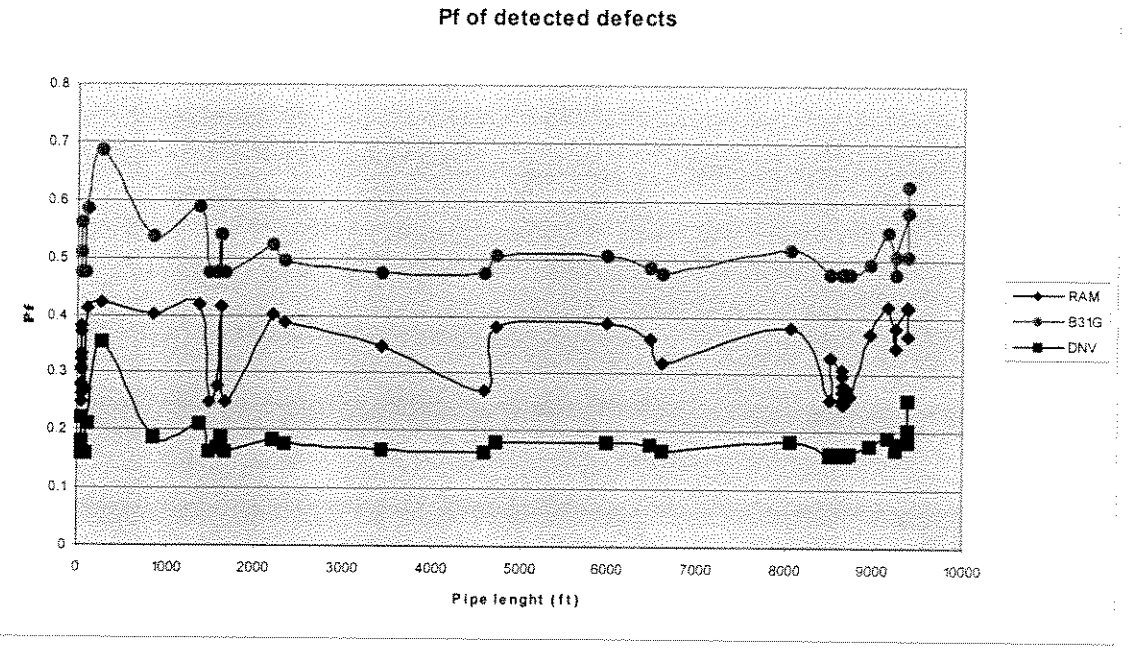

Fig 7: Pf of detected defects from the three models.

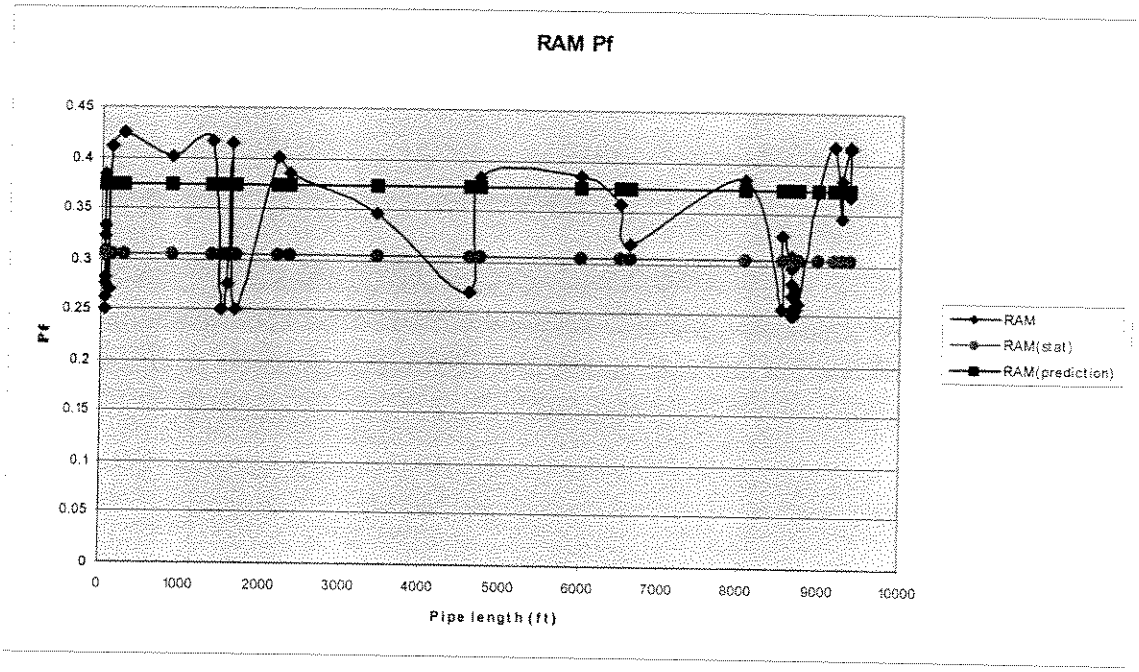

Fig 8: RAM Pf for detected and non-detected defects.

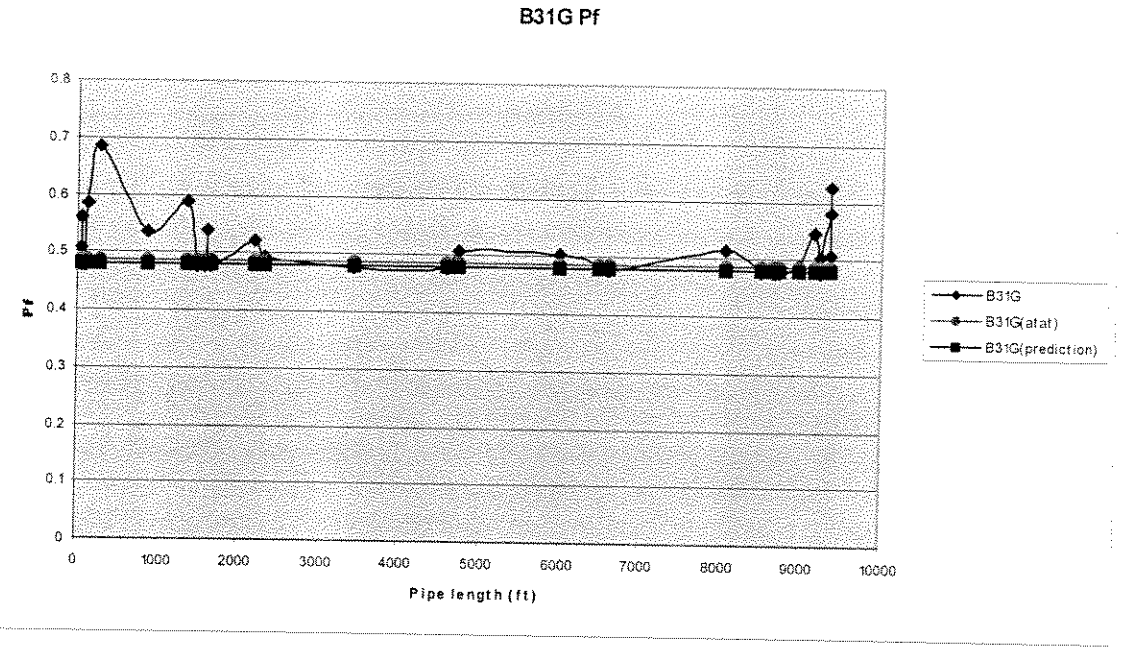

Fig 9: B31G Pf for detected and non-detected defects.

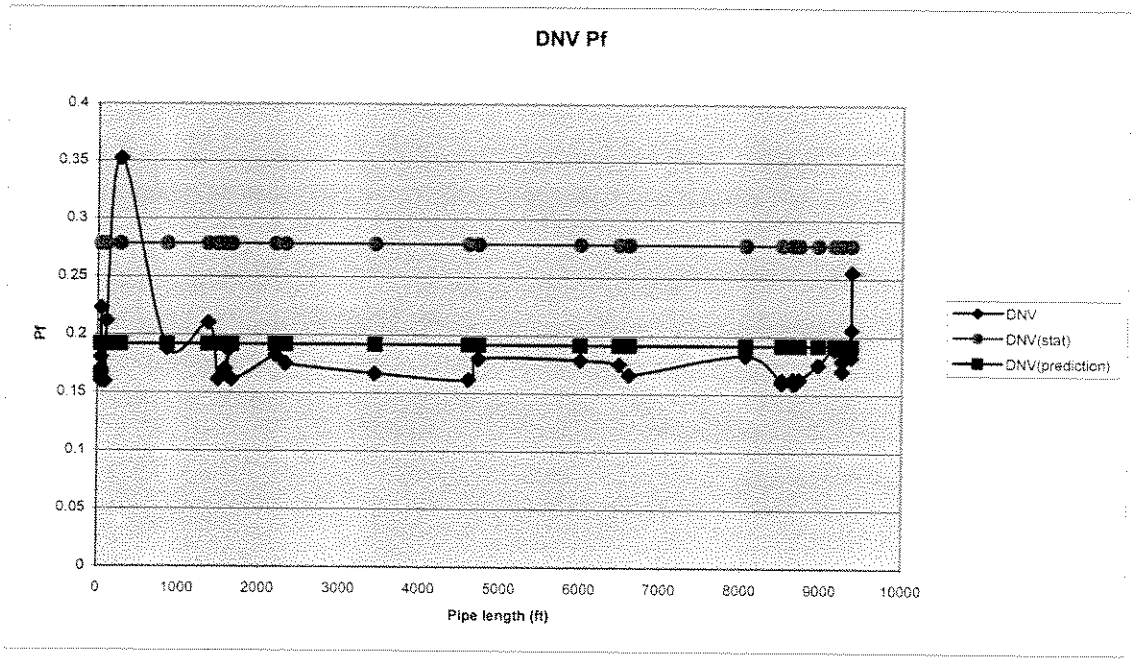

Fig 10: DNV Pf for detected and non-detected defects.

VI) Final analysis

A) Analysis

The consistent results of the test (section V) confirm that the program is "functional".

The program integrates most of the researched factors that affect the reliability of pipelines. It also presents a useful tool to calculate the probability of failure with different models and for all sections of the pipeline (detected and non-detected defected). The approach used in this research to assess the effects of the probabilities of detection/ non-detection is a unique approach and among the very few for pipelines in-line inspection tools.

However, and in order to account for all the parameters, lot of complexities have been added to the program to integrate the many aspects researched to affect the reliability of the pipelines which render it slightly complicated for both users and programmers, especially that it has been developed using excel. This complexity could be avoided by doing a parametric study to "filter" the important parameters that considerably affect the probability of failure in order to simplify the task for both users and programmers.

Other researches should complement this work whether on the technical aspect or on other parallel aspects. In order to build on this research, which I believe is a very strong start, which might lead to very important outcomes, I suggest the following:

B) Recommendations:

To improve the developed program:

- Perform a parametric study to select the most "useful" information that affect the most the reliability of the pipelines
- Based on the outcomes of the parametric study, modify program to only account for those factors qualified impotents by the parametric study in order to make the program more user and programmer friendly.
- Work on the "format" of the program by the use of a more advanced programming tool/language, which will simplify the algorithms and the user "feedback".
- A close cooperation between a professional programmer and the developer of this excel program is highly recommended for proper communication of algorithms used and technical information's the professional programmer does not usually have.

- This program has lots of potentials to be developed and implemented by large industries.
- Account for uncertainties related to pig location along the pipeline.

To improve the technical aspects:

- Develop and research more corrosion rates models.
- Correct corrosion models by the use of more statistics.
- Work to understand and incorporate better the different forms of corrosions.
- Develop more accurate information on POD and detections uncertainties.

To account for important complementary aspects:

- Analyze the effects of human and organizational factors on pipelines integrity and reliability. Large errors might occur from processing pig data information.
- Implement models to plan inspection policies, and link it to cost of inspections and cost of failures.
- Use corrosion models to predict the inspection policies and when to carry them.
- Corrected the corrosion models after every inspection with field data and reiterate to get new inspection policies.

VII) Conclusion

This research presented a large variety of subjects of importance to pipelines integrity and reliability. It presented some of the various models used to assess the burst pressures of pipelines and illustrates their use, and revealed their relative accuracies and biases. It also provided information on probability of detection/ non-detection for in-line instrumentation pigs, and their relative uncertainties. The topic of corrosion rates was also addressed, and concepts of probability theory and pipeline reliability were introduced.

The current report, with the development of the excel program, integrate most of the aspects of the topics covered during this research project. Some aspects however still need to be further researched and than integrated for reliability calculations.

Finally, we believe that this research project is a strong foundation toward many developments in the field of offshore pipelines and in-line instrumentations techniques, and that industries can built on it to develop useful and optimal inspection policies for purposes of risks assessments and managements of their infrastructures.

References

Alder, Henry L. and Roessler, E.B., Introduction to Probability and Statistics, W. H. Freeman and Company, San Francisco: 1960.

ASME B31G, Manual For Determining the Remaining Strength of Corroded Pipelines, American Society of Mechanical Engineers, New York: 1986

Bea et al. Performance of Offshore Pipelines Report. May 2001

Bea et al. Real-Time Risk Assessment. Summer 2000

Bea, R.G. Load Engineering. (Course Reader), Copy Central, Berkeley, 1995.

Bea, R.G., "Real-Time Risk Assessment and Management of Pipelines," Summer 2001 Report, Berkeley, 2001.

Bea, R.G, "Reliability Analysis & Management of Corrosion of Marine Pipelines", National association of Corrosion Engineers, 2002.

Bea, R.G., and Xu, Tao, "Evaluation of Biases and Uncertainties in Reliability Based Pipeline Requalification Guidelines," Proceedings of Pipeline Requalification Workshop, OMAE Conference: 1999.

Bubenik, Tom, Nestleroth, J.B., et. al. "Introduction to Smart Pigging in Natural Gas Pipelines," Report to the Gas Research Institute, Batelle, Ohio: 2000.

Beuker, Thomas, Personal Communication

Beuker, T.M. and B. W. Brown, et. al., "Advanced Magnetic Flux Leakage Signal Analysis for Detection and Sizing of Pipeline Corrosion Field Evaluation Program," A report by H. Rosen Engineering, for The Gas Research Institute, Houston: 1999

Det Norske Veritas, "Recommended Practice Corroded Pipelines," Norway, 1999.
Farkas, Botond, and Bea, R.G., "Risk Assessment and Management of Corroded Offshore Pipelines," UC Berkeley, Berkeley: 1999.

J.R. Benjamin, C.A. Cornell, Probability, Statistics, and Decision for Civil Engineers, McGraw-Hill Inc., New York: 1970

Jansen, H.J.M, Festen, M.M. : "Intelligent pigging developments for metal loss and crack detection", insight, Vol 137, 6, 1995, pp421.

Jansen, H.J.M, Van de Camp, P.J.B, Geerdink, M.: Magnetization as a key parameter of magnetic flux leakage pigs for pipeline inspection", Insight, Vol 136, 9, 1994, pp 672.

Kim, Sang and Bea, R.G., "Real-Time Risk Assessment and Management of Pipelines," Summer 2000 Report, Berkeley, 2000.
Lewis. Introduction to Reliability Engineering. New York. 1987

McLelland, Angus and Bea, R.G., "Real-Time Risk Assessment and Management of Pipelines," Spring 2001 Report, Berkeley, 2001.

Nestleroth, J.B., Rust, S.W, Burgoon, D.A.: "determining Corrosion Defect Geometry from Magnetic Flux Leackage Pig Data", Proceedings of NACE annual conference, paper 44, 1996, p44/1-44/11.

Shell International Exploration and Production B.V., "Specification and Requirement for Intelligent Pig Inspection of Pipelines, Version 2.1, 6 November 98.

Inspectech webpage, ; last accessed 05/17/2002
http://www.inspectech.ca/Papers/Flux2/

The e-journal of non-destructive testing: last accessed 05/17/2002
http://www.ndt.net/article/ecndt98/reliabil/325/325.htm

The e-journal of non-destructive testing: last accessed 05/17/2002
http://www.ndt.net/article/0498/forli/forli.htm

Battelle webpage, last accessed 05/17/2002.
http://www.battelle.org/pipetechnology/MFL/MFL98Main.html

The American Society for Non-destructive Testing webpage: last accessed 05/17/2002
http://www.asnt.org/publications/materialseval/basics/jan98basics/jan98basics.htm

Appendix

Appendix a) User Guidelines:

All inputs are to be entered in "sheet1"of the spreadsheet. Data required to input have the cells colored. The following data have to be inputted:

1. For the different specified feature types (General pitting, pitting defect, axial grooving, circumferential grooving) and for different defect depth intervals (intervals of 10% of thickness t from 0 to t) the user should enter the following:
    - POD: Under columns B,F, J, N, Which is the probability of detection given a call, in other term, the cumulative probability that given a call, the call is true, i.e, a defect exist. This data should come from inspection companies and tool vendors.
      Typical values of d for a POD of 90% are:
        - General defect: 0.1t.
        - Pitting defect: 0.2t
        - Axial Grooving: 0.15t
        - Circumferential Grooving: 0.15t
    - The median depth as a fraction of thickness t: Ranges from 0 to t at 0.1t increments. Under columns C, G, K, O. This is needed in order to correct for measurement errors and bias between data from the pig, and the real value of the depth of the defect. Inspection companies should have a database on the bias and distribution of the measured depth. User has to enter the "real" defect depths corresponding to the measured depth. Ex: when a pig measures a defect depth of 0.1t, the real median depth of the defect is 0.11t (this is the value to be inputted).
      Typical values of median measured depth vs real depth:
      For a real depth of 0.2t, the measured depth is 0.22t.
      For a real depth of 0.8t, the measured median depth is 0.77t.
    - The coefficient of variation of the defect depth d and that of tc (tc = t-d) remaining thickness): Under columns D, E, H, I, L, M, P, Q(The reason behind inputting for both d and tc is to avoid truncations close to t and 0t of the assumed lognormal distribution. Both are used when appropriate in the algorithm to minimize "lost are" outside 1t.
      Typical values of coefficient of variations for d are 10% for d= 0.2t and 20% for d=0.8t.

2. Input respectively for W (width) and L (length) of defects the following:

- The median W or L as a fraction of t: Under columns S (median Width) and V (median Length) for the correction purposes explained for the defect depth.
  Typical values of L and W: 2t to 6t.
  For a real value of 3t, W and L measured around 3.2t.
- The coefficient of variation of W and L: Under columns T and W.
  Typical values: 10 to 20%.

Note: Data inputted under (1) and (2) are to be provided by pig vendors and inspection companies, and may be a company or a tool (pig) characteristics, thus this data need to be imputed once as long as the same tool is being used. Moreover the typical values used are for purpose of illustration as well as to give an approximate "sense" for engineers. More exact values are to be required as mentioned from inspection companies.

3. Pig Run data or feature characteristics:
   - Position of the pig in the pipeline inputted in ft: under Column X.
   - Depth, width, and length of defect in fraction of t: under columns Y(depth), Z(width), and AA(length).
     Typical values: d = 0.5t, W and L = 4t.
4. Pipe data:
   - Median and V (coefficient of variation) for:
     - Thickness (in): typical values of 0.3 inches and V of 10%. (Columns AB, AC).
     - SMYS (ksi): Typical values of 40 Ksi and V of 10%. (AD, AE).
     - SMTS (ksi): Typical values of 52 Ksi and V of 10%. (AF, AG).
     - Outside Diameter D (in): Typical values of 8 inches And V of 10%. (AH, AI).

5. Pressure data (ksi):
   - Median and V: Typical values 2 ksi and V of 10%. (AJ, AK).

6. Bias:
   - Median and V for Capacity Bias:
     - RAM pipe: bias (B) =1, V= 34%. (AL, AM).
     - B31-G: B = 1.52, V = 36%. (AN, AO).
     - DNV: B = 1.48, V = 57%. (AP,AQ).
   - Median and V for Demand bias:
     Not studied enough. Assumed B =1 and V = 0. (AR, AS, AT, AU, AV, AW).

7. Predicted or expected median defect depth, width and length from corrosion models and their respective coefficients of variations:
   - Median and V for d (in): Function of the age, the conditions of the pipeline as well as the prediction model used. Under columns (BA,BB).
   - Median and V for W (in): Function of the age, the conditions of the pipeline as well as the prediction model used. Under columns (BA, BB).

- Median and V for L (in): Function of the age, the conditions of the pipeline as well as the prediction model used. Under columns (BA, BB).

Appendix b) Developed spreadsheets and calculations.

Sample Inputs:

Measured	Real data for General pitting				Real data for Pitting defect			
d (X*t)	POD	Median d	Vd(fraction)	Vtc(fraction)	POD	Median d	Vd(fraction)	Vtc(fraction)
0	1	0	0	0	1	0	0	0
0.1	1	0.1	0	0	1	0.1	0	0
0.2	1	0.2	0	0	1	0.2	0	0
0.3	1	0.3	0	0	1	0.3	0	0
0.4	1	0.4	0	0	1	0.4	0	0
0.5	1	0.5	0	0	1	0.5	0	0
0.6	1	0.6	0	0	1	0.6	0	0
0.7	1	0.7	0	0	1	0.7	0	0
0.8	1	0.8	0	0	1	0.8	0	0
0.9	1	0.9	0	0	1	0.9	0	0
1	1	1	0	0	1	1	0	0

Table 1: Inputs for POD and defect depth uncertainties

Real data for Axial Grooving				Real data for Circumferential grooving			
POD	Median d	Vd(fraction)	Vtc(fraction)	POD	Median d	Vd(fraction)	Vtc(fraction)
1	0	0	0	1	0	0	0
1	0.1	0	0	1	0.1	0	0
1	0.2	0	0	1	0.2	0	0
1	0.3	0	0	1	0.3	0	0
1	0.4	0	0	1	0.4	0	0
1	0.5	0	0	1	0.5	0	0
1	0.6	0	0	1	0.6	0	0
1	0.7	0	0	1	0.7	0	0
1	0.8	0	0	1	0.8	0	0
1	0.9	0	0	1	0.9	0	0
1	1	0	0	1	1	0	0

Table 2: Inputs for POD and defect depth uncertainties

W (X*t)	median W	V(W)	L (X*t)	median L	V(L)	Distance (ft)	Depth(X*t)	width(X*t)	Length(X*t)
0	0	0	0	0	0	39.505	0.250	2.126	3.308
0.5	0.5	0	0.5	0.5	0	39.739	0.120	2.048	3.308
1	1	0	1	1	0	39.781	0.100	1.732	2.678
1.5	1.5	0	1.5	1.5	0	40.124	0.150	2.284	4.330
2	2	0	2	2	0	40.138	0.230	2.44	3.150
2.5	2.5	0	2.5	2.5	0	40.195	0.190	2.914	3.780
3	3	0	3	3	0	40.199	0.120	2.284	2.756
3.5	3.5	0	3.5	3.5	0	40.439	0.120	1.968	2.834
4	4	0	4	4	0	40.454	0.370	2.204	3.386
4.5	4.5	0	4.5	4.5	0	40.696	0.120	2.756	4.174
5	5	0	5	5	0	40.717	0.100	1.812	1.732
5.5	5.5	0	5.5	5.5	0	41.945	0.200	1.968	3.150
6	6	0	6	6	0	42.185	0.100	1.968	2.440
6.5	6.5	0	6.5	6.5	0	42.371	0.140	1.89	2.520
7	7	0	7	7	0	43.692	0.340	2.204	7.560
7.5	7.5	0	7.5	7.5	0	44.441	0.230	2.678	3.228
8	8	0	8	8	0	92.421	0.130	2.678	1.102
8.5	8.5	0	8.5	8.5	0	111.863	0.450	1.496	4.724
9	9	0	9	9	0	275.545	0.490	2.362	11.968
9.5	9.5	0	9.5	9.5	0	856.807	0.420	2.834	3.544
10	10	0	10	10	0	1361.224	0.470	2.284	4.410
10.5	10.5	0	10.5	10.5	0	1486.085	0.100	2.126	2.598
11	11	0	11	11	0	1569.664	0.140	0.866	5.040
11.5	11.5	0	11.5	11.5	0	1611.383	0.460	2.756	3.150
12	12	0	12	12	0	1653.234	0.100	2.204	2.520
12.5	12.5	0	12.5	12.5	0	2194.626	0.420	2.52	3.150
13	13	0	13	13	0	2320.538	0.380	1.89	2.834
13.5	13.5	0	13.5	13.5	0	3427.530	0.280	1.26	2.440
14	14	0	14	14	0	4592.774	0.130	1.812	2.362
14.5	14.5	0	14.5	14.5	0	4717.281	0.370	2.44	3.308
15	15	0	15	15	0	5983.869	0.380	1.654	3.150

Table 3: Inputs for width and depth corrections, and pig data about pipe

Pipe data							
t nominal(in)		SMYS (ksi)		SMTS(ksi)		diameter D(in)	
median	V(fraction)	median	V(fraction)	median	V(fraction)	median	V(fraction)
0.5	0.12	42	0.08	52	0.08	8.625	0.1

Table 4: Pig data

Pressure data

Median (ksi)	V(fraction)
5.186	0.1
5.186	0.1
5.186	0.1

Table 5: Demand data

Capacity bias					
RAM		B31G		DNV	
Median	V	Median	V	Median	V
1	0.34	1.52	0.36	1.48	0.57

Table 6: Capacity bias

Demand bias					
RAM		B31G		DNV	
Median	V	Median	V	Median	V
1	0	1	0	1	0

Table 7: Demand Bias

Median d(in)	V
0.17	0.2

Median W(in)	V
0.5	0.2

Median L(in)	V
0.5	0.2

Table 8: Predictions for defect depth, width, length and their correspondent coefficients of uncertainties from corrosion models

Sample outputs:

Detected defects		
Pf		
RAM	B31G	DNV
0.332882	0.474889	0.17072
0.263048	0.474889	0.163842

0.249622 0.474889 0.161752
0.281437 0.474889 0.168773

Table 9: detected defects Pf from the three models.

Median d(in) V
0.0975 0.56135

Median W(in) V
0.9255 0.310245

Median L(in) V
1.496 0.546877

Table 10: Statistics values for depth, width and length.

	Pf	
RAM	B31G	DNV
0.306121	0.487983	0.277938

Table 11: Non-detected defects Pf from statistics and with the three models.

	Pf	
RAM	B31G	DNV
0.374538	0.479984	0.191606

Table 12: Non-detected defects Pf from predictions and with the three models.

Appendix c) Data for the report calculations.

Line 25 data.

DISTANCE [ft.]	MAX. DEPTH [%.]	LEN [in.]	WID [in.]	
39.505	25	1.063	1.654	
39.739	12	1.024	1.654	
39.781	10	0.866	1.339	
40.124	15	1.142	2.165	
40.138	23	1.220	1.575	
40.195	19	1.457	1.890	
40.199	12	1.142	1.378	
40.439	12	0.984	1.417	
40.454	37	1.102	1.693	
40.696	12	1.378	2.087	
40.717	10	0.906	0.866	
41.945	20	0.984	1.575	
42.185	10	0.984	1.220	
42.371	14	0.945	1.260	
43.692	34	1.102	3.780	
44.441	23	1.339	1.614	
92.421	13	1.339	0.551	
111.863	45	0.748	2.362	
233.649				
275.545	49	1.181	5.984	
856.807	42	1.417	1.772	
1361.224	47	1.142	2.205	
1486.085	10	1.063	1.299	
1569.664	14	0.433	2.520	
1611.383	46	1.378	1.575	
1653.234	10	1.102	1.260	
2194.626	42	1.260	1.575	
2320.538	38	0.945	1.417	
3427.530	28	0.630	1.220	
4592.774	13	0.906	1.181	
4717.281	37	1.220	1.654	
5983.869	38	0.827	1.575	
6475.969	31	0.984	1.693	

6597.481	22	0.591	1.417
8052.064	37	0.748	1.811
8506.312	11	0.709	0.827
8506.404	24	0.709	0.866
8643.035	18	0.472	0.827
8643.807	15	0.551	1.181
8643.955	11	0.591	0.906
8644.392	13	0.512	0.709
8644.596	20	0.709	1.063
8645.677	10	0.906	0.630
8647.784	10	0.906	1.024
8648.032	10	0.551	0.827
8648.291	13	0.787	0.945
8649.605	11	0.433	0.866
8675.925	11	0.394	0.709
8676.029	14	0.827	0.945
8719.087	12	0.984	1.496
8956.595	34	0.709	1.575
9158.235	47	1.339	1.614
9245.991	28	0.827	1.496
9245.998	37	0.551	1.614
9364.101	47	0.709	2.087
9364.195	46	0.591	3.465
9364.195	33	1.102	1.969

Appendix d) Corrosion information

Burst Pressure Analysis: Corroded Pipe

For pipeline corrosion defects not detected by the pig during its run, the level of corrosion can be predicted using a corrosion prediction model. The internal loss of wall thickness due to corrosion was predicted, based on a corrosion prediction model:

Loss of pipeline wall thickness due to corrosion (Bea, et.al., OTC, 1998):

$$t_c = t_{ci} + t_{ce}$$

Where:

t_c = total loss of wall thickness
t_{ci} = internal corrosion
t_{ce} = external corrosion

$$tc_i = \alpha_i \cdot \nu_i \cdot (L_s - L_p)$$

t_{ci} = loss of wall thickness due to internal corrosion
α = effectiveness of the inhibitor or protection
ν = average corrosion rate
L_s = average service life of the pipeline
L_p = life of the initial protection provided to pipeline

Internal Inhibitor Efficiency, α_i	
Descriptor	Inhibitor Efficiency
Very Low	10
Low	8
Moderate	5
High	2
Very High	1

Table 1: Internal Inhibitor Efficiency

Expected Life of Protective System (Lp), or Service Life of the Pipeline(Ls)	
Descriptor	Lp or Ls (years)
Very Short	1
Short	5
Moderate	10
Long	15
Very Long	>20

Table 2: Expected Life of Initial Protective System, or Service Life of Pipeline

Corrosion Rates and Variabilities		
Descriptor	Corrosion Rate, ν_t	Corrosion Rate Variability
Very Low	3.94E-5 in./year	10%
Low	3.94E-4 in./year	20%
Moderate	3.94E-3 in./year	30%
High	.0394 in./year	40%
Very High	.394 in./year	50%

Table 3: Corrosion Rates and Variabilities (Bea, et.al., OTC, 1998)

Pipeline Characteristics	
Wall Thickness, t (Inches)	0.322
Corrosion Characteristics	
Internal Inhibitor Effeciency, α_i	5
Expected Life of Protective System, Lp (Years)	10
Service Life of Pipeline, Ls (Years)	20
Corrosion Rate, ν_t (Inches/Year)	0.00394
Total Loss of Internal Wall Thickness (Inches)	0.197
Depth of Corrosion, d (Inches)	0.197
Loss of Wall Thickness as a Percent of Initial Wall Thickness, (d/t)	61%

Table 4: Sample calculation